SECURITY MARKING

The classified or limited status of this report applies to each page, unless otherwise marked.
Separate page printouts MUST be marked accordingly.

THIS DOCUMENT CONTAINS INFORMATION AFFECTING THE NATIONAL DEFENSE OF THE UNITED STATES WITHIN THE MEANING OF THE ESPIONAGE LAWS, TITLE 18, U.S.C., SECTIONS 793 AND 794. THE TRANSMISSION OR THE REVELATION OF ITS CONTENTS IN ANY MANNER TO AN UNAUTHORIZED PERSON IS PROHIBITED BY LAW.

NOTICE: When government or other drawings, specifications or other data are used for any purpose other than in connection with a definitely related government procurement operation, the U. S. Government thereby incurs no responsibility, nor any obligation whatsoever; and the fact that the Government may have formulated, furnished, or in any way supplied the said drawings, specifications, or other data is not to be regarded by implication or otherwise as in any manner licensing the holder or any other person or corporation, or conveying any rights or permission to manufacture, use or sell any patented invention that may in any way be related thereto.

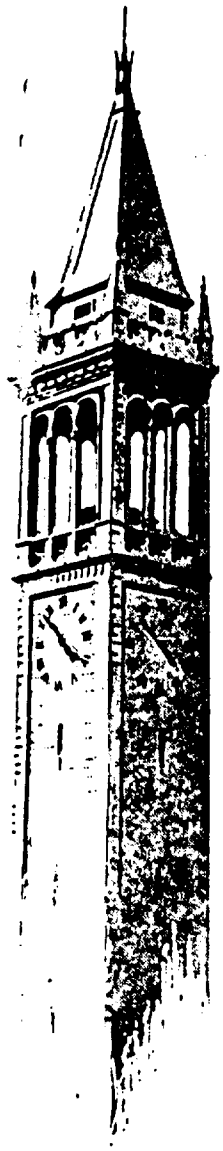

EXPANSION OF A PARTIALLY-IONIZED GAS THROUGH A SUPERSONIC NOZZLE

by

L. Talbot
Y. S. Chou
F. Robben

Report No. AS-65-14
AFOSR Grant 538-65
August 1965

INSTITUTE OF ENGINEERING RESEARCH

UNIVERSITY OF CALIFORNIA
Berkeley, California

GRANT 538-65
REPORT AS-65-14
AUGUST 1965

SPONSORED BY
THE AIR FORCE OFFICE OF
SCIENTIFIC RESEARCH

EXPANSION OF A PARTIALLY-IONIZED GAS THROUGH A SUPERSONIC NOZZLE

by

L. Talbot
Y. S. Chou
F. Robben

FACULTY INVESTIGATORS:
L. TALBOT, PROFESSOR OF AERONAUTICAL SCIENCES
F. S. SHERMAN, PROFESSOR OF AERONAUTICAL SCIENCES

SUMMARY

A theoretical investigation was made of the non-equilibrium expansion of a partially ionized gas through a supersonic nozzle. Both hydrogen and argon were studied. The ionization and recombination rate parameters used were those calculated by Bates and co-workers, using their collisional-radiative model of the recombination process. These calculations, for hydrogen, include the influence of radiation trapping on the overall rates, and yield as well the amount of recombination energy which is gained by the third-body electron in the recombination.

The energy balance for the electrons and massive particles was studied for both the optically thin (all recombination radiation lost) and optically thick (all radiation absorbed) cases. It was found that the recombination process produces an increase in electron temperature over that of the ion-atom temperature, and that this temperature difference is greater for the optically thick than for the optically thin case. Also, there is more net recombination for the optically thin case.

For high initial ionization (62%), recombination affects the gross flow variables measurably, when compared with the "frozen flow" solution. For low initial ionization (1%) the gross flow variables are practically unaltered, and the principal effect of the recombination is to produce an elevated electron temperature.

On comparing the hydrogen and argon flows, one finds that the effect of the larger atomic mass of the argon is to diminish the effectiveness of electron-atom energy exchange, resulting in a larger difference between electron and atom temperatures. For large initial ionization, the fractional amount of recombination in the supersonic part of the nozzle was greater in argon than in hydrogen, due to the longer residence time of the argon in the nozzle. But for low initial ionization, the reverse was true, because the higher electron temperature in the argon reduced the recombination rate.

Electron thermal conductivity effects were found to be unimportant for the frozen and non-equilibrium flows, but should be included in the equilibrium flow calculations.

1.0 INTRODUCTION

The purpose of the present paper is to present a detailed study of the flow of a partially-ionized gas through a convergent-divergent nozzle, taking into account electron-ion recombination and the radiative and collisionally-transferred energy liberated in the recombination. Considerable recent work has been done [1-7] which establishes the fact that in many recombining plasmas the recombination mechanism is dominantly electron-electron-ion three body recombination to a highly excited atomic level, followed by collisional and radiative de-excitation to the ground state. As a consequence of this process, one finds that a part of the potential energy of ionization is given to the third body electron, with the result that the temperature of the electron gas is elevated above that of neutral gas. The energy liberated in the form of radiation may or may not be re-absorbed by the neutral atoms, depending on the character of the plasma. An important feature of the recombination process is that the net recombination rate is strongly dependent on the electron temperature.

The collisional-radiative recombination model has been applied to the case of a decaying static plasma, and found to be in excellent agreement with experiment. [1,3] However, the consequences of the model have not yet been examined fully for a flowing plasma, in which there are strong coupling effects between the fluid dynamical phenomena and the recombination parameters. The purpose of the present paper is to investigate these effects. We have chosen to examine the consequences of the collisional-radiative recombination process in the rapid expansion of a partially ionized plasma through a supersonic nozzle. In particular, we are interested in how the inequality between electron and ion temperatures, which is a crucial factor in the recombination process, differs in the flow case from what is observed in a decaying static plasma. Also, we wish to ascertain how the flow is affected by the presence

or absence of radiation trapping. We have chosen hydrogen as our model gas, because the recombination theory is most complete in this case. However, we have also carried out approximate calculations for argon, in order to ascertain the influence of the atomic mass on the process.

The expansion of an ionized gas through a supersonic nozzle has been investigated by Bray and Wilson [8], Sockel [9], and others, without, however, including radiation losses. Bray and Wilson studied argon, and used a recombination rate coefficient deduced from the ionization rate given by Petschek and Byron [10]. This procedure is most appropriate for a highly ionized gas. Sockel used an approximate recombination rate formula taken from Hinnov and Hirschberg [1], which is valid for low electron temperatures ($kT_e \lesssim 0.25$ eV). Sockel also assumed the electron and atom-ion temperatures to be equal. Another study closely related to the present work is that of Byron, Bortz and Russell [19]. These authors have discussed in detail the important radiative processes and their influence on the collisional-radiative recombination rate, and have carried out several calculations on the flow of helium through a supersonic nozzle. We shall have more to say of this work later.

In the present work, values for the rate coefficients and radiation power are taken from the calculations of Bates, Kingston and McWhirter [4,5]. The general theory of these calculations can be found in the original papers, and will not be discussed here. For simplicity, two extreme cases regarding radiative power are considered. The first is the "optically-thin" case, denoted by $\sigma(\lambda) = 0$, where $\sigma(\lambda)$ is the optical thickness of the plasma at a wavelength λ. In this case, all the radiated energy is lost from the plasma. The other extreme is the optically thick case, $\sigma(\lambda) = \infty$, in which all the radiation is re-absorbed by the plasma. Generally speaking, cases of practical interest such as the plasma-jet flows fall somewhere between

these two extremes, as is pointed out by Byron, et.al.[19]. A typical situation [19] is where the plasma is optically thin to continuum radiation and transitions between excited states, but optically thick for transitions to the ground state. Bates, et.al., have in fact computed rate constants for this case, as well.

Throughout the analysis, the following assumptions are employed: The flow is taken to be quasi-one-dimensional. The self-relaxation times (the times for randomization of the thermal velocities) of all the species are much shorter than the characteristic flow time, so that the velocity distribution for each specie is Maxwellian (though not necessarily at the same temperature). Viscosity, mass diffusion and heat conduction effects are assumed to be absent. Axial heat conduction by the electrons is shown to be negligible by numerical examination of the final results. We also assume that the mass flow velocities of electrons, ions and neutral atoms are all equal, and that the ion and atom temperatures are the same. The equality of mass flow velocities implies that the net electrical current is zero, and that as a consequence an electric field between the ions and electrons must exist. This electric field plays a significant role in the electron energy balance, and acts to equalize the temperatures between the ions and electrons.

The mean free paths for collisions between species are all assumed to be much smaller than the characteristic flow length (say, the nozzle throat diameter) so that continuum flow equations are applicable. Lateral diffusion and wall recombination are neglected, and it is assumed that no applied magnetic or electric fields exist. Also, the ideal gas equation of state is taken for all species, and the additive law of partial pressures is employed.

Equilibrium solutions based on the Saha equation for electron density, and "frozen-flow" solutions are also presented for comparison with the

finite-rate calculations. Strictly speaking, one can have neither equilibrium nor frozen flow for the $\sigma = 0$ case, because in this case the flow is not adiabatic. However, in the case $\sigma = \infty$ the equilibrium and frozen flow solutions should represent the two limiting cases.

2.0 GOVERNING EQUATIONS

We take u to be the flow velocity, x the distance measured along the nozzle axis, whose local cross-sectional area is A, and we let N_e, N_i, N_a be the electron, ion and atom number densities, respectively. The conservation of electron number density is expressed by

$$A \frac{\partial N_e}{\partial t} = \frac{\partial}{\partial x} (N_e A u) \tag{2.1}$$

and the global continuity equation is

$$\frac{d}{dx} (\rho u A) = 0 \tag{2.2a}$$

where

$$\rho = N_a m_a + N_i m_i + N_e m_e \approx (N_a + N_e) m_a \tag{2.2b}$$

We have assumed the ionic and atomic masses to be equal, $m_i = m_a$, and have invoked the condition of plasma neutrality $N_i = N_e$. The global momentum equation is

$$\rho u \frac{du}{dx} = - \frac{dp}{dx} \tag{2.3a}$$

where we take for the total pressure

$$p = p_i + p_a + p_e \approx (N_i + N_a) kT + N_e kT_e \quad , \tag{2.3b}$$

making use of the ideal gas law approximation with $T_i = T_a = T$. In the above, k is Boltzmann's constant.

For the global energy equation we have

$$u \frac{d}{dx}\left(i + \frac{1}{2} u^2 \right) = - \frac{R}{\rho} \tag{2.4a}$$

in which

$$i = \frac{e}{\rho} + \frac{p}{\rho} \tag{2.4b}$$

is the enthalpy per unit mass, and R is the power lost by radiation, per unit volume. If X is the ionization energy per atom, then the internal energy per unit volume is

$$e = \frac{3}{2} \{N_e \, kT_e + (N_a + N_i) \, kT\} + N_e X$$

and the enthalpy and pressure can be written as

$$i = \frac{5}{2} \frac{k}{m_a} (T + f \, T_e) + \frac{f}{m_a} X \tag{2.5a}$$

$$p = \frac{\rho}{m_a} k(T + f \, T_e) \tag{2.5b}$$

where the degree of ionization is defined as

$$f = \frac{N_e}{N_a + N_e} \tag{2.6}$$

Equations (1) and (2) combine to give

$$\rho \frac{u}{m_a} \frac{df}{dx} = \frac{\partial N_e}{\partial t} \tag{2.7}$$

The rate equation which determines $\partial N_e / \partial t$ is, in the collisional-radiative model of Bates, Kingston and McWhirter [4],

$$\frac{\partial N_e}{\partial t} = - \alpha N_e^{\,2} + S \, N_e \, N_a \tag{2.8}$$

in which α and S are the recombination and ionization rate constants. It may be noted that the term involving S is important only when the electron

density is near Saha equilibrium. From (2.7) and (2.8), we obtain

$$\frac{df}{dx} = -[(\alpha + S)f - S]\frac{N_e}{u} \tag{2.9}$$

One more equation is needed to complete the formulation of the problem, an electron energy balance relationship. This is given, for a recombining plasma, by

$$\rho_e u \frac{d}{dx}\left(i_e + \frac{1}{2}u^2\right) - Fu = -\left(\frac{5}{2}kT_e + \chi\right)\left(\frac{\partial N_e}{\partial t}\right) - R - Q_{ei} - Q_{ea} \tag{2.10}$$

Here F is the force exerted on the ions by the electrons, due to the induced electric field which is required to maintain $u_i = u_e = u$; hence Fu is the rate at which "flow work" is expended by the electrons. The first two terms on the right hand side of (2.10) together represent the net rate of energy gain of the electron gas due to the three-body recombination process, it being the total recombination energy rate less the power lost by radiation. The quantities Q_{ei} and Q_{ea} represent energy loss rates due to electron-ion and electron-atom collisions, respectively. For Q_{ei}, we use the expression given in Ref. 10,

$$Q_{ei} = \frac{N_e^2 e^4}{m_a}\left(\frac{8\pi m_e}{kT_e}\right)^{1/2}\left(\frac{T_e - T}{T_e}\right)\ln\left[\frac{9(kT_e)^3}{8\pi N_e e^6}\right] \tag{2.11}$$

in which e is the electronic charge. If we assume that the intermolecular force between electrons and atoms follows the inverse fifth-power law, then from Ref. 11

$$Q_{ea} = 2.5\frac{\pi}{m_a}(m_e B)^{1/2} k N_e K_a (T_e - T) \tag{2.12}$$

where B, the intermolecular force constant, will be taken from experimental data. (See Appendix B.)

The force F acting on the electrons can be evaluated from the electron momentum equation,

$$\rho_e u \frac{du}{dx} = - \frac{dp_e}{dx} + F + P_{ie} + P_{ae} \tag{2.13a}$$

where P_{ie} and P_{ae} represent momentum transfers due to collisions between electrons and massive particles. These terms vanish, however, if the assumption $u_i = u_e = u_a$ is made. Now, the electron pressure will in general be of the same order as the gas pressure p, but $\rho_e u(du/dx)$ will be of order $(m_e/m_a)\rho(du/dx)$. Hence to good approximation, we may write

$$F \cong \frac{dp_e}{dx} \tag{2.13b}$$

with neglect of terms of order (m_e/m_a); this relation implies that the force acting on the electrons which balances the electron pressure gradient is the induced electric field E set up between the ions and electrons in order to maintain $u_i = u_e$. Exactly the same conclusion, of course, follows from a consideration of Ohm's law (cf. Spitzer, Ref. 12, p. 28), if the conduction current is set equal to zero and in fact $F = N_e e E$. It has been pointed out by Morse, Mitchner and Kruger [13] that in order for Eq. (2.13b) to apply the nozzle must be insulated, otherwise the induced electric field would be shorted out. Equation (2.13b) still could be valid for a conducting nozzle, if the plasma were separated from the nozzle wall by a non-conducting boundary layer.

On substitution of Eqs. (2.11), (2.12) and (2.13b) into (2.10) and neglecting $\frac{1}{2} u^2$ as small compared to i_e, we obtain

$$\frac{dT_e}{dx} = \frac{2}{3} \frac{T_e}{\rho} \frac{d\rho}{dx} - \frac{\left(T_e + \frac{2}{3} \frac{\chi}{k}\right)}{f} \frac{df}{dx} - \frac{2 m_a R}{3\rho f u k}$$

$$- \frac{\rho}{u} \left[D_1 f T^{-3/2} \ln \left(\frac{D_2 T^3}{\rho f} \right) + (1 - f) D_3 \right] (T_e - T) \tag{2.14}$$

in which

$$D_1 = \frac{2e^4}{3m_a^2 k}\left(\frac{8\pi\, m_e}{k}\right)^{1/2} \quad ; \quad D_2 = \frac{9k^3 m_a}{8\pi e^6}$$

$$D_3 = \frac{5\pi (m_e B)^{1/2}}{3m_a^2} \qquad (2.15)$$

The problem is now completely formulated, and consists of the governing equations (2.2a), (2.3a), (2.4a), (2.9) and (2.14), together with the state equations (2.5). The quantities α, S and R are taken from the tables of Bates, et.al.[4]. The first two quantities, for the case $\sigma = \infty$, are plotted in Fig. 1, and compared with the values used by Bray and Wilson [8,15]. Analytical representations for these quantities are presented in Appendix A of this report.

3.0 THE ELECTRON TEMPERATURE EQUATION

It is of interest to form a differential equation for the electron-ion temperature difference $(T_e - T)$. By combining Eqs. (2.3a), (2.4a), (2.5) and (2.14), one obtains

$$\frac{d}{dx}(T_e - T) = -\frac{2}{3}\frac{m_a R}{\rho u f k} - \frac{1}{f}\left(T_e + \frac{2}{3}\frac{\chi}{k}\right)\frac{df}{dx} + \frac{2}{3}\frac{d\,\ell n\, p}{dx}\cdot(T_e - T)$$

$$- \rho\,\frac{(1+f)}{u}\left[D_1 f\, T^{-3/2}\,\ell n\left(D_2\frac{T_e^3}{\rho f}\right) + (1-f)\,D_3\right](T_e - T) \qquad (3.1)$$

Now, if there is no recombination, so that R and df/dx are zero, the formal solution of (3.1) can be written down as

$$(T_e - T) = C \exp\left[\int D\, dx\right] \qquad (3.2a)$$

where C is a constant and

$$D = \frac{2}{3}\frac{d(\ell n\, p)}{dx} - \rho\frac{(1+f)}{u}\left[D_1 f\, T^{-3/2}\, \ell n\left(\frac{D_2 T_e^{\,3}}{\rho f}\right) + (1-f)\, D_3\right] \tag{3.2b}$$

From (3.2) we see that if $T_e = T$ initially at $x = 0$, then $C = 0$ and T_e will remain equal to T throughout the expansion. This conclusion is valid provided heat conduction effects are negligible, as discussed later on. If on the other hand, the net recombination rate is not zero, then the electron gas will gain energy due to the recombination process, and T_e will in general be greater than T. The first two terms on the right of (3.1) together give the net rate of energy gain of the electrons. On the other hand, the negative pressure gradient acts to decrease the temperature difference $(T_e - T)$, as does collisional energy exchange between the electrons and the massive particles. These effects are represented by the third and fourth terms on the right of (3.2), respectively. Therefore, the resultant rate of change of $(T_e - T)$ represents a balance between the energy gain and energy loss mechanisms, and is determined by their relative effectiveness.

The effectiveness of collisional energy exchange is directly proportional to ρD_1 and ρD_3, which we see from (2.15) vary inversely with m_a. Thus, the larger the atomic mass, the less effective will be the energy exchange between the electrons and the ions and atoms, and we expect therefore that the temperature difference $(T_e - T)$ will be larger in an argon than in a hydrogen expansion. This expectation is borne out by the calculations. The pressure gradient term also acts to equalize the two temperatures, but its effect is small owing to the logarithmic dependence. On the other hand, if the expansion is rapid, the factor ρ/u multiplying the collisional exchange term decreases rapidly, diminishing the effectiveness of collisional equalization of the temperatures. The net result is that the more rapid is the expansion, the larger is the temperature difference.

The net electron energy gain depends on the rate of recombination and the amount of energy radiated away. Loss of recombination energy by radiation diminishes the amount of this energy which is given to the electrons, thus reducing the electron temperature. However, the recombination rate coefficient increases ($\alpha \sim T_e^{-9/2}$, according to the approximate analytical representation of Hinnov and Hirschberg [1]), so a decrease in electron temperature increases the rate of energy release, thus tending to drive the electron temperature in the opposite direction. As we shall see, radiation loss actually turns out to decrease the temperature difference $(T_e - T)$.

4.0 EQUILIBRIUM AND FROZEN FLOW EQUATIONS

Before proceeding to the finite-rate calculations, we shall discuss the two limiting cases of equilibrium and frozen flow. In equilibrium flow, the ion and electron temperatures are everywhere equal, and the degree of ionization is given by the Saha equation, which is

$$N_a = N_e^e \left(\frac{h^2}{2\pi m_e kT_e} \right)^{3/2} \left[\frac{g_a}{g_i g_e} \right] \exp\left(\frac{\chi}{kT_e} \right) \tag{4.1a}$$

where g is the quantum mechanical statistical weight. When numerical values for hydrogen are inserted, we obtain

$$\ell n \left(\frac{f^2}{1 - f^2} \right) = -1.195 - \ell n\, p + 2.5\, \ell n\, T - \frac{1.577 \times 10^5}{T} \tag{4.1b}$$

where p is the numerical value of the pressure in dyne/cm^2 and T is numerically equal to the temperature in °K. Since no energy is radiated away, the energy equation becomes

$$\frac{d}{dx}\left(i + \frac{u^2}{2} \right) = 0 \tag{4.2}$$

Using (4.2), (2.5), (2.3) and (4.1a), we arrive at the rate equation in the form

$$\frac{df}{dx} = \frac{6.308 \times 10^4 \, f(1 - f^2) \, \frac{d \ln p}{dx}}{\left[2T + f(1 - f) \left(T + 0.4 \, \frac{\chi}{k} \right) \left(2.5 + \frac{1.577 \times 10^5}{T} \right) \right]} \qquad (4.3)$$

Equations (4.1) and (4.2) together with (2.2), (2.3), (2.5) and (2.6) specify the equilibrium flow problem.

For frozen flow, $f = f_o$ = constant, $R = 0$ and $T_e = T$. The governing equations are then (2.2), (2.3), (2.5), (2.6) and (4.2).

5.0 METHOD OF SOLUTION

If we completely specify the nozzle contour in advance, the frozen and equilibrium flow solutions can be calculated directly, but it is necessary to iterate on the finite-rate equations in order to find the value of the mass flux which for a given set of inlet conditions yields sonic flow at the nozzle throat. Since the finite-rate equations are the most complicated, it is preferable to use a scheme which allows these equations to be solved directly, and perofrm the iterations on the equilibrium- and frozen-flow equations instead. This can be accomplished by specifying, for the finite-rate equations, the pressure distribution in the convergent portion of the nozzle, and computing with this pressure distribution until sonic flow is reached. Beyond this point, in the supersonic portion of the nozzle, A(x) can be prescribed. In the course of the calculation, A(x) in the subsonic portion of the nozzle is determined from the continuity equation. Iterations on the initial conditions for the equilibrium and frozen flow equations are carried out until sets of values are found which give sonic flow at the throat of the same nozzle shape as was determined from the finite-rate solution.

For the pressure distribution in the convergent section, we selected a dependence of the form $p = p_o \, e^{-bx^2}$, where p_o is the inlet pressure

and b is a parameter to be chosen. The inlet conditions are not stagnation conditions, but rather correspond to a large but finite area A_o and a small but finite approach Mach number M_o. In the divergent section, the area ratio was chosen to be of the form

$$A = A_* + K(x - x_*)^2 \tag{5.1}$$

where A_* is the throat area, $K = \pi \tan^2 \theta$, and x_* the distance from the inlet to the throat. The divergent section thus asymptotes to a conical nozzle with half-angle θ. Figure 2 shows the nozzle contour which resulted from this method of calculation for the chosen values $\theta = 15°$ and $b = 1\ cm^{-2}$.

Then, for given p(x), the governing equations for non-equilibrium flow can be written as:

$$\frac{df}{dx} = -[(\alpha + S)f - S]\frac{\rho f}{m_a u} \equiv F_1 \tag{2.9}$$

$$\frac{d\rho}{dx} = \frac{\frac{3}{5}\cdot\frac{dp}{dx} + \frac{2}{5}\frac{R}{u} + \frac{2}{5}\frac{\rho\chi}{m_a}F_1}{\frac{k}{m_a}(T + f\,T_e)} \equiv F_2 \tag{5.2}$$

$$\frac{dA}{dx} = \frac{A}{\rho u^2}\frac{dp}{dx} - \frac{A}{\rho}F_2 \tag{5.3}$$

$$\frac{du}{dx} = -\frac{1}{\rho u}\frac{dp}{dx} \tag{2.3}$$

$$\frac{dT_e}{dx} = \frac{3}{2}\frac{T_e}{\rho}F_2 - \frac{[(5/3)T_e + \chi/k]F_1}{f} - \frac{2\,m_a R}{3\,\rho\,k\,f\,u}$$

$$- \frac{\rho}{u}\left[D_1 f\,T_e^{-3/2}\,\ell n\left(\frac{D_2 T_e^{\,3}}{\rho f}\right) + (1 - f)\,D_3\right](T_e - T) \tag{2.14}$$

For given A(x), Eqs. (2.3), (2.9) and (2.14) remain unchanged. Equation (5.2) is replaced by

$$\frac{du}{dx} = \frac{\frac{2}{3}\frac{R}{\rho u^2} + \frac{5}{3}\frac{k}{u\, m_a A}(T + f\, T_e)\frac{dA}{dx} + \frac{2}{3}\frac{\chi}{u\, m_a}\frac{df}{dx}}{1 - \frac{5}{3}\frac{k}{m_a u^2}(T + f\, T_e)} \equiv F_2' \tag{5.4}$$

and instead of (5.2) we use

$$\frac{d\rho}{dx} = -\frac{\rho}{A}\frac{dA}{dx} - \frac{\rho}{u}F_2' \tag{5.5}$$

The equations for equilibrium flow are obtained by setting $R = 0$, $T_e = T$, and replacing (2.9) by (4.3).

For frozen flow, if we specify $p = p_o e^{-bx^2}$, the equations can be integrated and one obtains

$$\frac{A}{A_o} = \frac{(5/3)M_o^2 e^{(3/5)bx^2}}{1 + (5/3)M_o^2 - e^{(-2/5)bx^2}} \tag{5.6}$$

$$\frac{\rho}{\rho_o} = e^{(-3/5)bx^2} \tag{5.7}$$

$$u^2 = \frac{5p_o}{\rho_o}\left[1 - e^{(-2/5)bx^2}\right] + u_o^2 \tag{5.8}$$

$$x_*^2 = \frac{5}{2b}\ln\left[\frac{4}{3 + M_o^2}\right] \tag{5.9}$$

and hence, from the condition $(dA/dx) = 0$ at $x = x_*$,

$$\frac{A_*}{A_o} = \frac{\frac{5}{3}M_o^2\left[\frac{4}{3 + M_o^2}\right]^{3/2}}{1 + \frac{5}{3}M_o^2 - \left(\frac{3 + M_o^2}{4}\right)} \tag{5.10}$$

The Mach number M_o is defined as

$$M_o = \frac{u_o}{\sqrt{\frac{5}{3}kT_o(1 + f_o)}} \tag{5.11}$$

If M_o is small, we see from (5.9) that x_* depends only on the parameter b. Also, from (5.10), we observe that (A_*/A_o) is independent of b and a function only of M_o. These properties serve as a guide in the choices of M_o and b for a desirable inlet shape in the non-equilibrium flow problem. For different flow conditions, b and M_o have to be adjusted so as to keep the convergent portion of the nozzle the same.

In the actual frozen flow calculations, the solutions given by Eqs. (5.6) - (5.10) were not used, because the specification $p = p_o e^{-bx^2}$ was introduced to avoid iteration in the non-equilibrium case. The frozen flow solution can be obtained, of course, by integrating the equations for a given A(x) determined from the non-equilibrium solution. This integration can be carried out in closed form, with the result

$$\left(\frac{Q_o p_o^{-2/5} - 5}{Q_o p^{-2/5} - 5}\right)^{1/2} \left(\frac{p_o}{p}\right) = \frac{A(x)}{A_o} \tag{5.12}$$

$$\left(\frac{\rho}{\rho_o}\right) = \left(\frac{p}{p_o}\right)^{3/5} \tag{5.13}$$

$$u^2 = u_o^2 + 5\frac{p_o}{\rho_o}\left[1 - \left(\frac{p}{p_o}\right)^{2/5}\right] \tag{5.14}$$

where

$$Q_o = \frac{\rho_o u_o^2}{p_o^{3/5}} + 5\, p_o^{2/5} \tag{5.15}$$

and T is given by the equation of state. It was, however, found more convenient to compute the frozen flow solution by numerical integration of the differential equations than by numerical evaluation of the algebraic relations (5.12) - (5.15).

All of the calculations were performed on an IBM 7094 computer. The Adams four-point integration formula was used.

6.0 RESULTS AND DISCUSSION

The cases which were computed are tabulated in Table I. The inlet conditions in all cases were chosen to correspond to Saha equilibrium, although other conditions could have been used. If the gas were arc-heated at low pressure, for instance, it might very well not be in Saha equilibrium. The non-equilibrium inlet conditions would depend in a complicated way on the experimental arrangement, and would probably have to be measured experimentally. The inlet parameters were chosen principally to illustrate the results of the analysis, although the low ionization case perhaps is somewhat representative of arc-heated wind tunnel performance. Ideally, it would have been desirable to compute enough cases to permit parametric representation of the results from which one could obtain the flow properties corresponding to any given set of inlet conditions within a useful range. However, the numerical integrations were too laborious and time-consuming to make this feasible, and we contented ourselves with the examination of essentially two cases, representative of the weakly ionized and the highly-ionized regimes.

The argon calculations were performed primarily to illustrate the influence of atomic mass on the recombination coefficient, and it was assumed that the same values of α and S as used for hydrogen would be applicable to argon. For α, this assumption should be quite good as long as the electron density is not too high. Although several arguments can be advanced to support this point of view, the most direct is the classical calculation of three-body recombination carried out by Makin and Keck [20]. These results are in agreement with the quantum mechanical calculations of Bates, and are equally valid for argon as for hydrogen, as they consider only classical electron orbits around a charged core. It might be noted that the much larger recombination rates for argon reported by Byron, Bortz and Russell [19] were the result of over-estimating the unknown collisional

transition probabilities, and it is now generally agreed that Bates' hydrogen values for α should be reasonably accurate for argon as well [22]. The values of S for argon should be much smaller than for hydrogen, because of the higher first excitation potential, but S is only important in the region upstream of the sonic throat when conditions are near Saha equilibrium, and thus very little error is made in the properties in the supersonic region, where the flow becomes highly non-equilibrium. The radiated power R, which enters into the electron energy balance given by Eq. (2.10), should be chosen so that the net energy of recombination given up to the free electrons is the same for argon as for hydrogen in the optically thin case. We thus find that

$$R_{argon} = R_{hydrogen} - (\chi_{A} - \chi_{H}) \frac{dN_e}{dt} \quad .$$

In the actual calculations R_{argon} was chosen to be a slightly smaller value, so that the fraction of recombination energy given to the free electrons was about 16 percent larger than that given above. Thus in the argon calculations the electron temperature is a little higher than it should be, but the difference is quite small, and less than the uncertainties of the model of recombination used.

The results are presented in Figs. 3 - 11. The curves are double-valued functions of A/A_* because properties in both the subsonic and supersonic portions of the nozzle are plotted. The gross flow properties, ρ, u, p and f are shown in Figs. 3 - 6. We observe from Fig. 3 that for $f_o = 0.62$, and $\theta = 15°$ in hydrogen, the density variations for the two non-equilibrium cases and for frozen flow are essentially indistinguishable. The density falls more rapidly for the equilibrium flow, however. Equivalent information is presented in Figs. 4a and 4b, where the flow velocities are plotted. Although not discernable on the graphs, the velocity for $\sigma = 0$ is slightly greater than

that for $\sigma = \infty$. The highest velocity is obtained for frozen flow, and the lowest for equilibrium flow.

Computed pressure variations in the nozzle are shown in Figs. 5a and 5b. As in the case of the velocity and density, not much difference is found between the non-equilibrium and frozen flows. The pressure in equilibrium flow remains somewhat higher than the other cases, throughout the supersonic portion of the nozzle, for $f_o = 0.62$. For the low initial ionization, $f_o = 0.01$, the pressure variations for all cases are practically identical, as might have been expected.

Figure 6 shows the variation in fractional ionization f, for initial condition $f_o = 0.62$. The effect of expansion angle is what one expects; increasing θ moves the flow closer to the frozen limit, and vice versa. The non-equilibrium finite-rate flows are much closer to frozen flow than to equilibrium flow. The actual electron number densities in the nozzle are plotted in Figs. 7a, 7b and 7c. It can be seen that for the low initial ionization case, $f_o = 0.01$, the equilibrium flow calculation gives an extremely rapid drop in N_e. One notes that the "sudden-freezing" model [21] which has been used successfully for atomic recombination would be a poor approximation for electron-ion recombination, as has been previously observed by Bray [15] and Byron, et.al.[19].

Some of the most interesting results of the calculations are presented in Figs. 8a, 8b, 8c and 9, where the electron and ion-atom temperatures are plotted. In Fig. 8a, we see that the temperatures for the non-equilibrium cases in hydrogen are closer to frozen flow than to equilibrium flow, and the effect of increasing the expansion angle is to move the flow closer to the frozen limit, as one might have anticipated. The temperature level for $\sigma = \infty$ is higher than for $\sigma = 0$, as is the temperature difference $T_e - T$.

We observed that more recombination occurs for $\sigma = 0$, so that more recombination energy is liberated for this case. However, this recombination energy is largely lost by radiation, with the result that the gas temperature is lower for the optically thin case than for the optically thick case. The temperature difference $T_e - T$ is larger for the optically thick case because the effectiveness of energy transfer between electrons and ions is proportional to $T_e^{-3/2}$, and T_e is larger for the optically thick case. Thus radiation power loss serves both to increase the amount of recombination and cool the gas, while decreasing the temperature difference $T_e - T$. Similar comments apply to the data plotted in Fig. 8b. Although the gross flow variables are practically unaffected by recombination, for $f_o = 0.01$ we observe that there is a significant effect on T_e due to radiation absorption.

The temperature behavior of argon is shown in Fig. 8c. Here we observe that for $f_o = 0.01$, the gas temperature T is hardly affected by the presence or absence of recombination. However, T_e at the exit of the nozzle $(A/A_* = 100)$ is almost an order of magnitude greater than T. As in the case of hydrogen, the difference $(T_e - T)$ is greater for the optically thick case than for the optically thin case. For similar conditions, this temperature difference $(T_e - T)$ is larger in argon than in hydrogen. This is because the energy exchange rate between electrons and massive particles is inversely proportional to the atomic mass m_a, as seen from Eqs. (2.11) and (2.12). The data for $(T_e - T)$ have been replotted in Fig. 9 to show this effect more clearly.

Another comparison between the behavior of argon and hydrogen, in terms of the fractional amount of recombination, is shown in Figs. 10a and 10b. Two competing effects are involved in determining the variation in $\Delta = (f_o - f)/f_o$. Since the flow velocities are lower in argon than in hydrogen, the residence

time in the nozzle is longer for the argon, and this tends to increase the net recombination. However, for reasons just discussed, the temperature difference $(T_e - T)$ is greater in argon, and the recombination rate is a strong inverse function of T_e. For the case of high initial ionization, $f_o = 0.62$, the residence-time effect predominates, and $\Delta_A > \Delta_H$ at large A/A_*, as seen in Fig. 10a. The converse occurs for low initial ionization, $f_o = 0.01$, as seen in Fig. 10b.

The Mach numbers obtained for the various cases are plotted in Figs. 11a and 11b. In general, the behavior is what might have been expected.

7.0 EFFECT OF HEAT CONDUCTION

It has been recognized [14,15] that the presence of high temperature electrons, even in small mole-fractional amounts, can increase the thermal conductivity of a gas markedly. In a rapid expansion through a nozzle, large axial temperature gradients are produced, and it is appropriate therefore to examine the effect of axial heat conduction on the energy balance.

The importance of axial heat conduction can be assessed by examining the value of the quantity

$$\Omega \equiv \frac{\frac{5}{2} N_e u k \frac{dT_e}{dx}}{\frac{d}{dx}\left(k_e \frac{dT_e}{dx}\right)}$$

which is the ratio of the net electron enthalpy flux and the electron heat flux out of a control volume. Conduction effects will be negligible if $\Omega \gg 1$.

For the electron thermal conductivity k_e, we use the value given by Spitzer [14] (pp. 144-145)

$$k_e = \epsilon \delta_T k_L$$

where

$$k_L = 20\left(\frac{2}{\pi}\right)^{3/2} \frac{(k'T)^5 k}{m_e^{1/2} e^4 \ell n \Lambda}$$

$$\Lambda = \frac{3}{2e^3}\left(\frac{k^3 T^3}{\pi n_e}\right)^{1/2}$$

In our case, $\epsilon = 0.419$ and $\delta_T = 0.225$. For a Lorentz gas, $f \ll 1$ and $\delta_T = 1$.

We have calculated Ω at $A/A_* = 10$ for the various cases. For hydrogen, we found

$f_o = 0.62$	$f_o = 0.01$
$(\Omega)_{\sigma=\infty} = 73$	$(\Omega)_{\sigma=\infty} = 12$
$(\Omega)_{\sigma=0} = 88$	$(\Omega)_{\sigma=0} = 18$
$(\Omega)_{\text{Frozen}} = 110$	$(\Omega)_{\text{Frozen}} = 27$
$(\Omega)_{\text{Equil}} \approx 1$	$(\Omega)_{\text{Equil}} \ll 1$

Similar numerical values are obtained in argon. Therefore, in all our examples involving finite rates and frozen flow, the neglect of heat conduction seems justified. For equilibrium flow, however, it appears that the conduction term must be included. One may conclude that in general the heat conduction term may be neglected except at very high electron temperatures or for very small degree of ionization. In the latter case, conduction effects would act to keep the electron temperature nearer to its initial value ahead of the expansion. These conclusions are essentially the same as those reached by Bray [15].

8.0 CONCLUDING REMARKS

We have not attempted any detailed comparisons between our argon results and those of Bray and Wilson [8,15], because the initial conditions taken by these authors differ from ours. However, one may remark that for the most part, their results and ours are qualitatively similar. The principal feature of our results which we believe is new is a more complete and accurate evaluation of the behavior of the electron and gas temperatures, and of the effects of radiation loss (as predicted for the optically thin case, $\sigma = 0$) on the overall recombination process. These effects may be summarized as follows: In comparing the two cases $\sigma = 0$ and $\sigma = \infty$, at a common station A/A_* in the nozzle, one finds that radiation loss (a) produces more cooling of the gas, (b) increases the net recombination, (c) decreases the temperature difference $(T_e - T)$ and (d) increases the expansion pressure ratio.

The effect of decreasing the expansion angle of the nozzle is to increase T_e and T, and increase the net recombination Δ, but to decrease the temperature difference $(T_e - T)$. All of these effects are traceable to the increase in residence time of the fluid in the nozzle.

For the case considered with initial ionization fraction $f_o = 0.62$, recombination effects alter the gross flow variables in the nozzle measurably though not dramatically. For the low initial ionization case, $f_o = 0.01$, the gross flow variables are essentially unaltered by the presence or absence of recombination, and the only significant result of the recombination is to maintain $(T_e - T) > 0$.

On comparing the argon and hydrogen flows, one finds that the effect of the larger atomic mass of the argon is to diminish the effectiveness of energy exchange between the electrons and massive particles, resulting in a larger temperature difference $(T_e - T)$ in argon. For the case $f_o = 0.62$,

the fractional amount of recombination Δ downstream in the supersonic portion of the nozzle was greater in argon than in hydrogen, because of the longer residence time of the argon in the nozzle. But for $f_o = 0.01$, Δ was greater in hydrogen, because the higher argon electron temperature reduces the recombination rate.

Electron thermal conductivity effects were found to be unimportant for the frozen and finite-recombination-rate flows, but should be included in equilibrium flow calculations, at least in the supersonic portion of the nozzle.

APPENDIX A

The rate constants and radiated power factors computed by Bates, et.al. are reported in tabular form at rather widely spaced intervals in N_e and T_e. For the numerical calculations of this report it was convenient to obtain an approximate analytical representation of these results. Since the Bates, et.al. results have a rather broad range of useful application, it seems worthwhile to report our analytical approximations.

It was found that the recombination coefficient α for $\sigma = 0$ could be represented adequately over range $500°K < 8000°K, 10^{12} \leq N_e \leq 10^{15}$ by the double series

$$\log_{10} \alpha = \sum_{i=0}^{3} \sum_{j=0}^{2} A_{ij} \left[\log_{10} \frac{N_e}{10^{12}} \right]^i \left(\frac{1000}{T_e} \right)^{j/2} \qquad (A.1)$$

The twelve coefficients A_{ij} were found by using Bates' tabular values and solving the resulting matrix equation; we obtained

$A_{00} = -13.825$	$A_{01} = 5.212$	$A_{02} = -0.7959$
$A_{10} = 0.05299$	$A_{11} = 0.7049$	$A_{12} = 0.06981$
$A_{20} = -0.14655$	$A_{21} = 0.6805$	$A_{22} = -0.458$
$A_{30} = 0.03$	$A_{31} = -0.1058$	$A_{32} = 0.07253$

Similarly, for the ionization rate S for $\sigma = 0$ we write

$$\log_{10} S = \sum_{i=0}^{2} \sum_{j=0}^{2} B_{ij} \left[\log_{10} \left(\frac{N_e}{10^{13}} \right) \right]^i \left(\frac{T_e}{4000} \right)^{j/2} \qquad (A.2)$$

In the range $T_e > 4000°K$, $N_e > 10^{12}$ cm^{-3}, we find the nine coefficients B_{ij} to be

$$B_{00} = -62.6086 \quad B_{01} = 51.004 \quad B_{02} = -12.8399$$
$$B_{10} = 2.1364 \quad B_{11} = -1.893 \quad B_{12} = 0.4810$$
$$B_{20} = -0.2685 \quad B_{21} = 0.4842 \quad B_{22} = -0.1542$$

For the power radiated, R, we write, for $\sigma = 0$,

$$R = R_o + N_e R_1 \tag{A.3}$$

where R_o corresponds to the quantity ${}^8P_o$ tabulated by Bates, et.al., and R_1 corresponds to their ${}^oR_1$.

We write

$$\log_{10} R_o = \sum_{i=0}^{3} \sum_{j=0}^{2} C_{ij} \left[\log_{10} \frac{N_e}{10^{12}} \right]^i \left(\frac{1000}{T_e} \right)^{j/2}$$
$$\log_{10} R_1 = \sum_{i=0}^{3} \sum_{j=0}^{2} D_{ij} \left[\log_{10} \frac{N_e}{10^{12}} \right]^i \left(\frac{T_e}{4000} \right)^{j/2} \tag{A.4}$$

and obtain

$$C_{00} = -0.5088 \quad C_{01} = 5.2306 \quad C_{02} = -0.8142$$
$$C_{10} = 2.1192 \quad C_{11} = 0.3779 \quad C_{12} = 0.3891$$
$$C_{20} = -0.2545 \quad C_{21} = 1.0944 \quad C_{22} = -0.8628$$
$$C_{30} = 0.0559 \quad C_{31} = -0.2108 \quad C_{32} = 0.1756$$

$$D_{00} = -48.924 \quad D_{01} = 38.89 \quad D_{02} = -10.07$$
$$D_{10} = -2.932 \quad D_{11} = 6.681 \quad D_{12} = -2.753$$
$$D_{20} = 3.352 \quad D_{21} = -5.684 \quad D_{22} = 2.337$$
$$D_{30} = -0.6826 \quad D_{31} = 1.158 \quad D_{32} = -0.4774$$

The range of applicability of R is approximately $500° < T_e < 16{,}000°$, $10^{12} < N_e < 10^{15}$.

For the optically thick case, $\sigma = \infty$, it is found that the dependence of α on N_e can be written explicitly as

$$\alpha_\infty = A_R + K_t N_e \tag{A.5}$$

On fitting Bates' tabulated values, we find

$$\log_{10} A_R = 182.333 - 1482.19 \left(\frac{1000}{T_e} \right)^{1/4} + 4455.599 \left(\frac{1000}{T_e} \right)^{1/2} - 6874.26 \left(\frac{1000}{T_e} \right)^{3/4} + 5786.5845 \left(\frac{1000}{T_e} \right) - 2530.238 \left(\frac{1000}{T_e} \right)^{5/4} + 450.16 \left(\frac{1000}{T_e} \right)^{3/2} . \tag{A.6}$$

$$\log_{10} K_t = 165.9957 - 1440.7328 \left(\frac{1000}{T_e} \right)^{1/4} + 4245.2524 \left(\frac{1000}{T_e} \right)^{1/2} - 6408.696 \left(\frac{1000}{T_e} \right)^{3/4} + 5299.7876 \left(\frac{1000}{T_e} \right) - 2285.3684 \left(\frac{1000}{T_e} \right)^{5/4} + 402.2243 \left(\frac{1000}{T_e} \right)^{3/2} . \tag{A.7}$$

This representation is valid over the range $250° < T < 16{,}000°$. The ionization rate for $\sigma = \infty$ can be expressed by the simple relation

$$S_\infty = 10^{-23.94} \left(\frac{T_e}{1000} \right)^{11.03} \tag{A.8}$$

in the range $8000° < T < 32{,}000°$.

APPENDIX B

Determination of the force constant B for the electron-atom interaction

The total collision cross-section for inverse fifth-power force law is given by (cf. Ref. 11)

$$\sigma_c = 2\pi(0.422)\left[\frac{(m_e + m_a)\,B}{m_e\,m_a}\right]^{1/2} g^{-1} \qquad (B.1)$$

where g is the relative velocity between electron and atom. To a good approximation, $g = \sqrt{3kT/m_e}$, the electron thermal speed. Then, since $m_e \ll m_a$, Eq. (B.1) reduces to

$$\sigma_c \simeq \frac{1.53\,B^{1/2}}{\sqrt{k\,T_e}} \qquad (B.2)$$

σ_c may also be expressed in terms of the collision probability P_c, following Ref. 16,

$$\sigma_c = 2.828 \times 10^{-17}\,P_c \qquad (B.3)$$

For hydrogen, from Ref. 17, we have for $kT_e \sim 1$ eV

$$\sigma_c = 28\,\pi\,a_o^2 \qquad (B.4)$$

where a_o is the radius of the first Bohr orbit. Inserting $\pi a_o^2 = 8.8 \times 10^{-17}$ cm^2, and comparing Eqs. (B.4) and (B.2) we obtain for hydrogen

$$B^{1/2} = 2.04 \times 10^{-21}\ erg^{1/2}\ cm^2 \qquad (B.5)$$

If we use this constant to calculate the quantity D_3 given by Eq. (2.1), we find that it agrees well with the value given in Ref. 7 for $T_e \simeq 1$ eV.

The collision probability P_c for argon has been measured by Brode [18], who found $P_c \simeq 3$ for $kT_e = 1$ eV. Using this value, we obtain for argon

$$B^{1/2} = 7 \times 10^{-23}\ erg^{1/2}\ cm^2 \quad . \qquad (B.6)$$

REFERENCES

[1] E. Hinnov and J. G. Hirschberg, "Electron-ion recombination in dense plasmas," Physical Review 3, 125 (1962), 795.

[2] S. Byron, R. C. Stabler, and P. I. Bortz, "Electron-ion recombination by collisional and radiative processes," Physical Review Letters 9, 8 (1962), 376.

[3] F. Robben, W. B. Kunkel, and L. Talbot, "Spectroscopic study of electron recombination with monatomic ions in a helium plasma," Physical Review 6, 132 (1963), 2363.

[4] D. R. Bates, A. E. Kingston, and R. W. P. McWhirter, "Recombination between electrons and atomic ions. I. Optically thin plasmas," Proceedings of the Royal Society A,267 (1962), 297.

[5] D. R. Bates, A. E. Kingston, and R. W. P. McWhirter, "Recombination between electrons and atomic ions. II. Optically thick plasmas," Proceedings of the Royal Society A,270 (1962), 155.

[6] D. R. Bates and A. E. Kingston, "Properties of a decaying plasma," Planetary & Space Science 1, 11 (1963).

[7] D. R. Bates and A. E. Kingston, "Recombination and energy balance in a decaying plasma. I. $H - H^+ - e$ plasma," Proceedings of the Royal Society A,279 (1964), 1310.

[8] K. N. C. Bray and J. A. Wilson, "A preliminary study of ionic recombination of argon in wind tunnel nozzles," AASU Report 185, University of Southampton, July (1961).

[9] P. M. Sockel, "Nonequilibrium expansion of a plasma from a thermionic source," National Aeronautics and Space Administration Technical Note D-2086, December (1963).

[10] H. Petschek and S. Byron, "Approach to equilibrium ionization behind strong shock waves in argon," Annals of Physics 1 (1957), 270.

[11] T. F. Morse, "Energy and momentum exchange between nonequipartition gases," Physics of Fluids 6 (1963), 1420.

[12] L. Spitzer, Physics of Fully Ionized Gases, 2nd Edition, Interscience (1962).

[13] F. H. Morse, M. Mitchner, and C. H. Kruger, "On a proposed mechanism for obtaining elevated electron temperatures," - to appear in Physics of Fluids.

[14] C. L. Brundin, L. Talbot, and F. S. Sherman, "Flow studies in an arc-heated low density wind tunnel," University of California Engineering Report HE-150-181 (1960).

[15] K. N. C. Bray, "Electron-ion recombination in argon flowing through a supersonic nozzle," in AGARDograph 68, "High temperature aspects of hypersonic flow," Pergamon Press (1963), Chapter 4.

[16] C. W. Allen, Astrophysical Quantities, 2nd Ed. The Athlone Press (1963).

[17] R. T. Brackmann, W. L. Fite, and R. H. Neynaber, "Collisions of electrons with hydrogen atoms. III. Elastic scattering," Physical Review 112 (1958), 1157.

[18] R. B. Brode, "The quantitative study of the collisions of electrons with atoms," Reviews of Modern Physics 5 (1933), 257.

[19] S. Byron, P. I. Bortz, and G. R. Russell, "Electron-ion reaction rate theory: determination of the properties of non-equilibrium monatomic plasmas in MHD generators and accelerators and in shock tubes," Proceedings of the 4th Symposium on the Engineering Aspects of Magnetohydrodynamics, University of California, Berkeley, April 10-11 (1963).

[20] B. Makin and J. C. Keck, "Variational theory of three-body electron-ion recombination rates," Physical Review Letters 11 (1963), 281.

[21] K. N. C. Bray, "Atomic recombination in a hypersonic wind tunnel nozzle," Journal of Fluid Mechanics 6 (1959), 1.

[22] S. Byron, Private communication.

TABLE I.

Gas	(a) Hydrogen	(b) Hydrogen	(c) Argon	(d) Argon
Non-Equilibrium				
f_o	0.62	0.01	0.669	0.01
N_{eo} cm^{-3}	1.0×10^{15}	4.79×10^{14}	1.04×10^{15}	4.66×10^{14}
p_o dyne cm^{-2}	4000	5.4×10^{4}	4000	5.4×10^{4}
ρ_o gm cm^{-3}	2.702×10^{-9}	8.03×10^{-8}	1.05×10^{-7}	3.122×10^{-6}
T_o °K	1.109×10^{4}	8.08×10^{3}	1.109×10^{4}	8.30×10^{3}
u_o cm sec^{-1}	7.86×10^{4}	5.25×10^{4}	1.265×10^{4}	8.42×10^{3}
M_o	0.050	0.0496	0.050	0.0496
b cm^{-2}	1.0	1.0	1.0	1.0
θ; $\sigma(\lambda)$	15°; $\sigma(\lambda) = 0,\infty$ 7.5; $\sigma(\lambda) = \infty$ 25°; $\sigma(\lambda) = 0$	15°; $\sigma(\lambda) = 0,\infty$	15°; $\sigma(\lambda) = 0,\infty$	15°; $\sigma(\lambda) = 0,\infty$
Equilibrium				
u_o cm sec^{-1}	6.9×10^{4}	4.9×10^{4}	1.063×10^{4}	7.34×10^{3}
M_o	0.050	0.0463	0.042	0.043
b cm^{-2}	0.77	0.77	0.77	0.77
θ	15°	15°	15°	15°
Frozen				
u_o cm sec^{-1}	7.92×10^{4}	5.36×10^{4}	1.276×10^{4}	8.50×10^{3}
M_o	0.050	0.050	0.050	0.050
θ	15°	15°	15°	15°

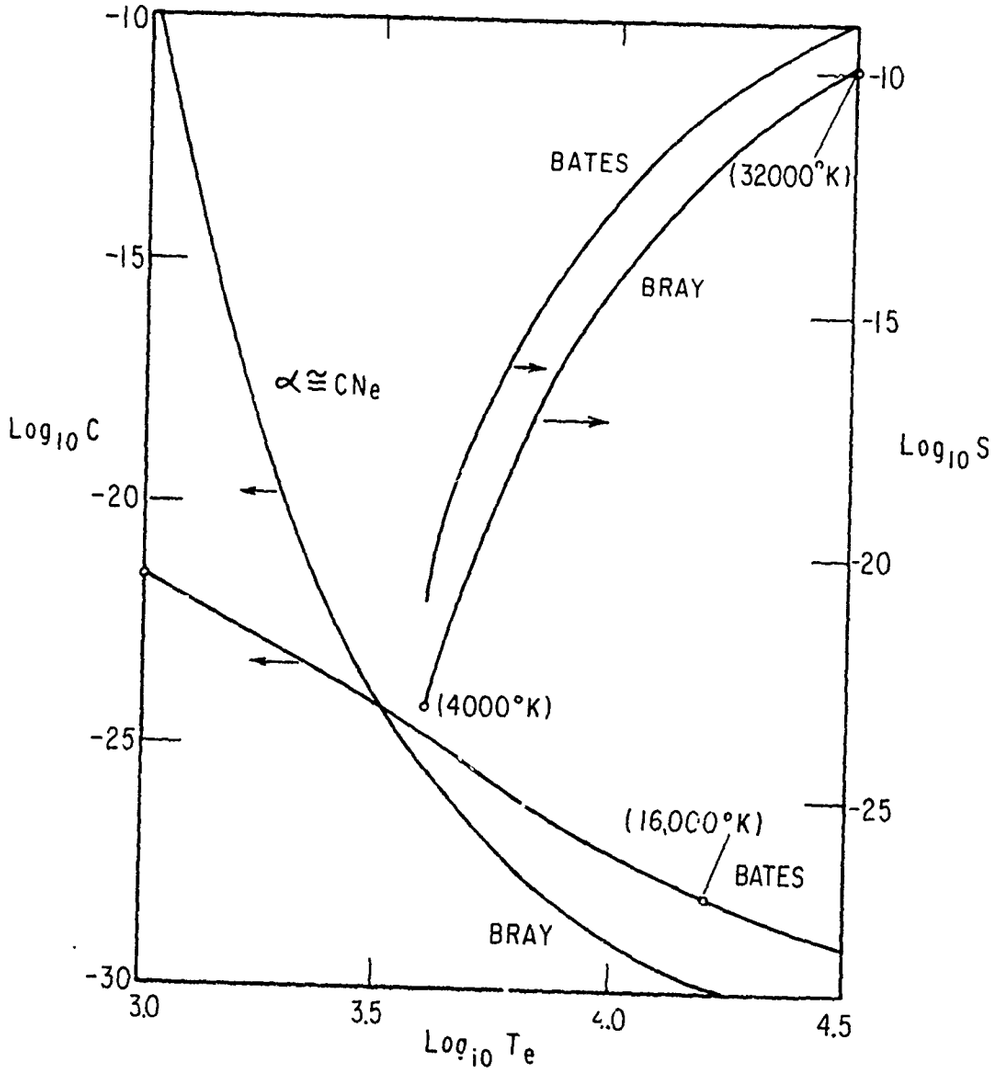

FIG 1 RATE CONSTANTS ($\sigma = \infty$)

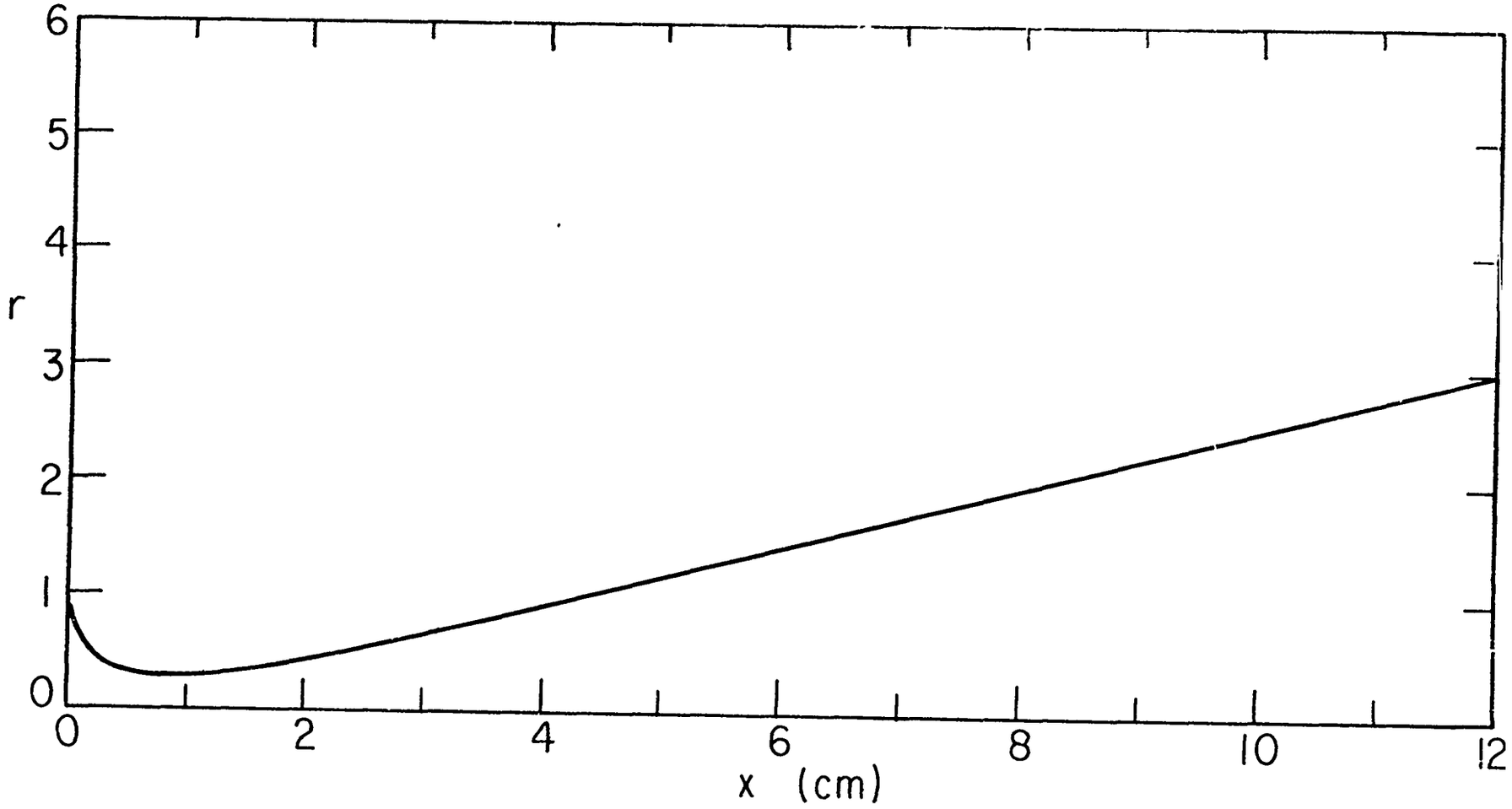

FIG. 2 NOZZLE CONTOUR, $\theta = 15°$

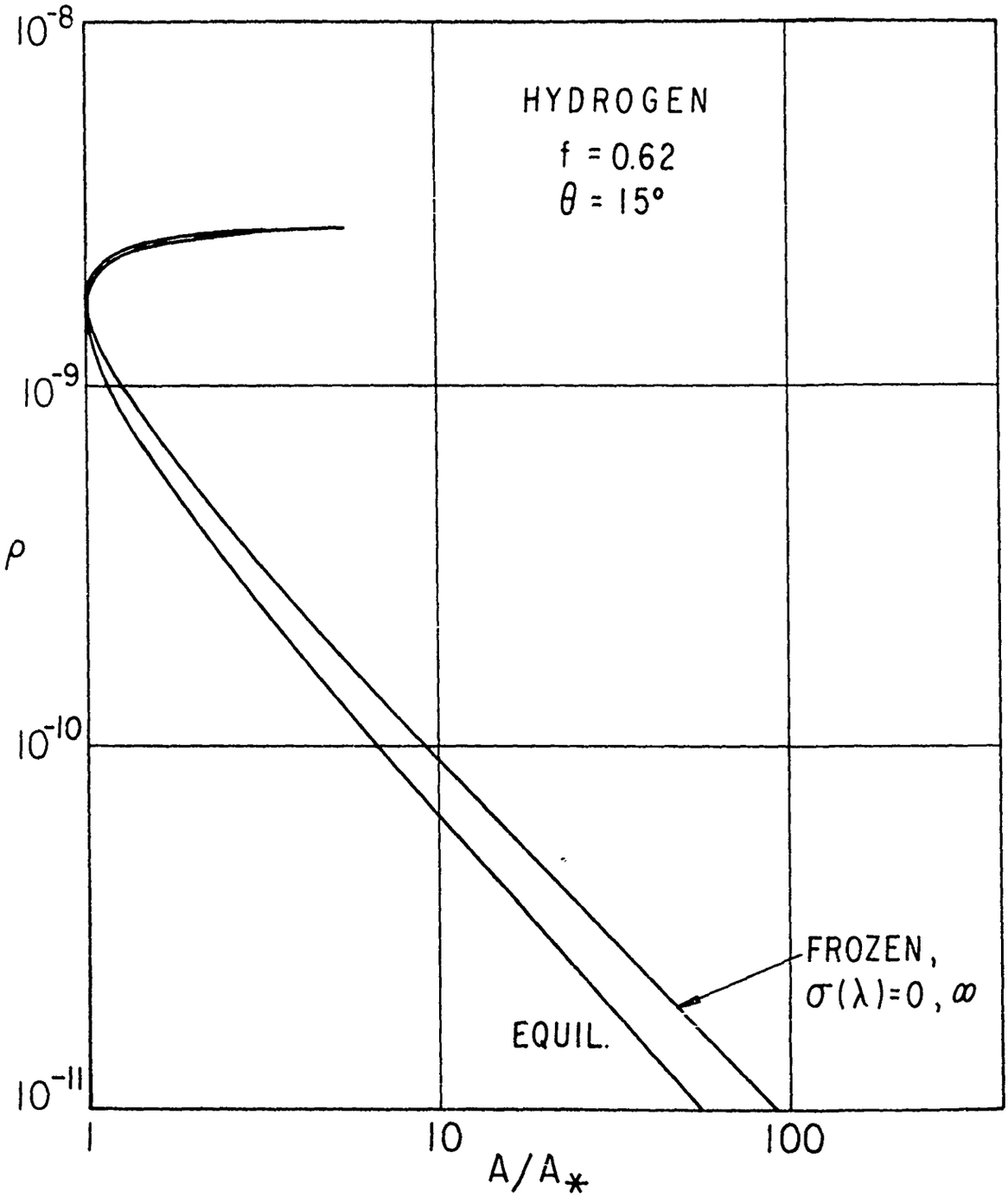

FIG. 3 DENSITY (gm/cm^3)

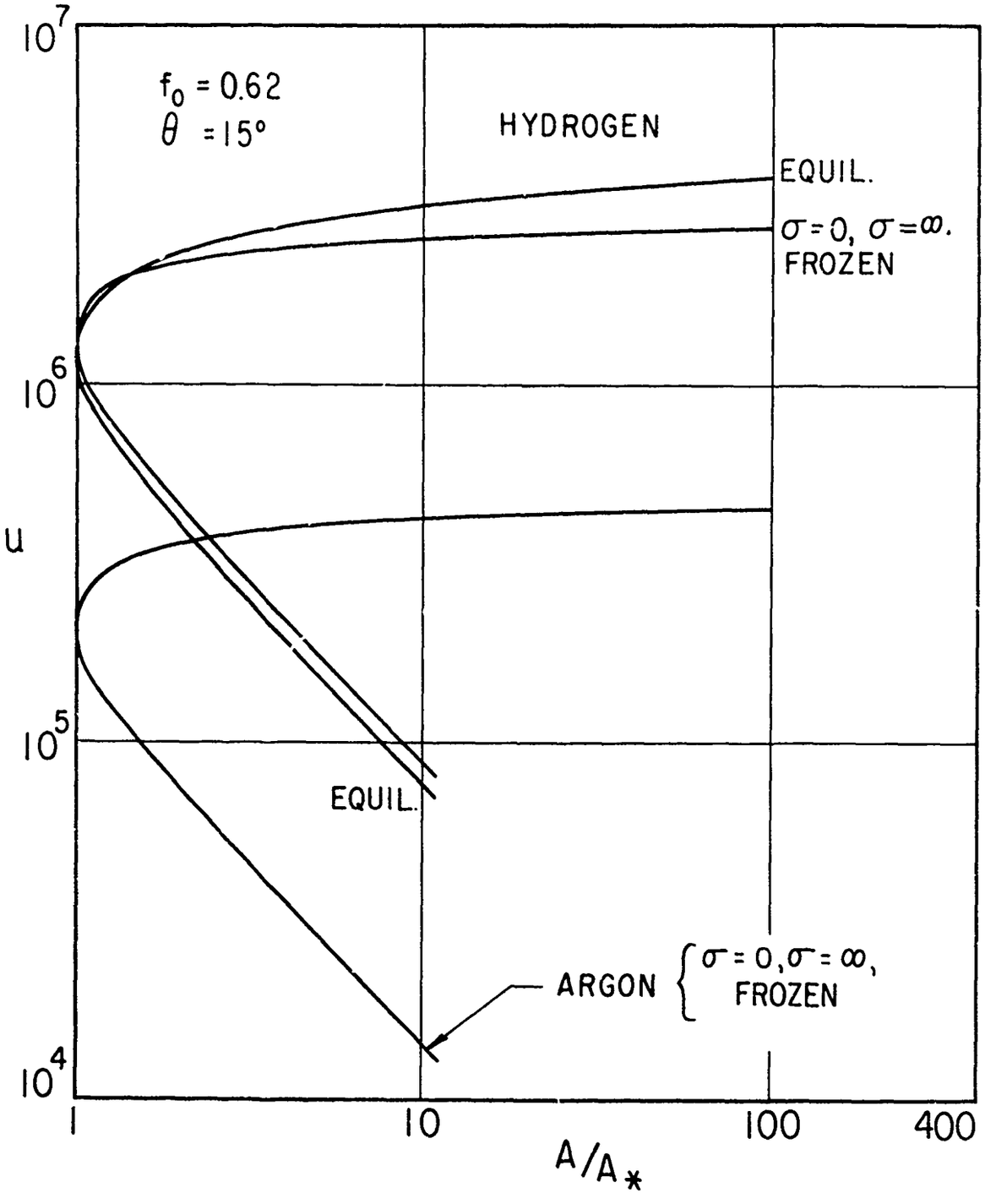

FIG. 4a VELOCITY (cm/sec)

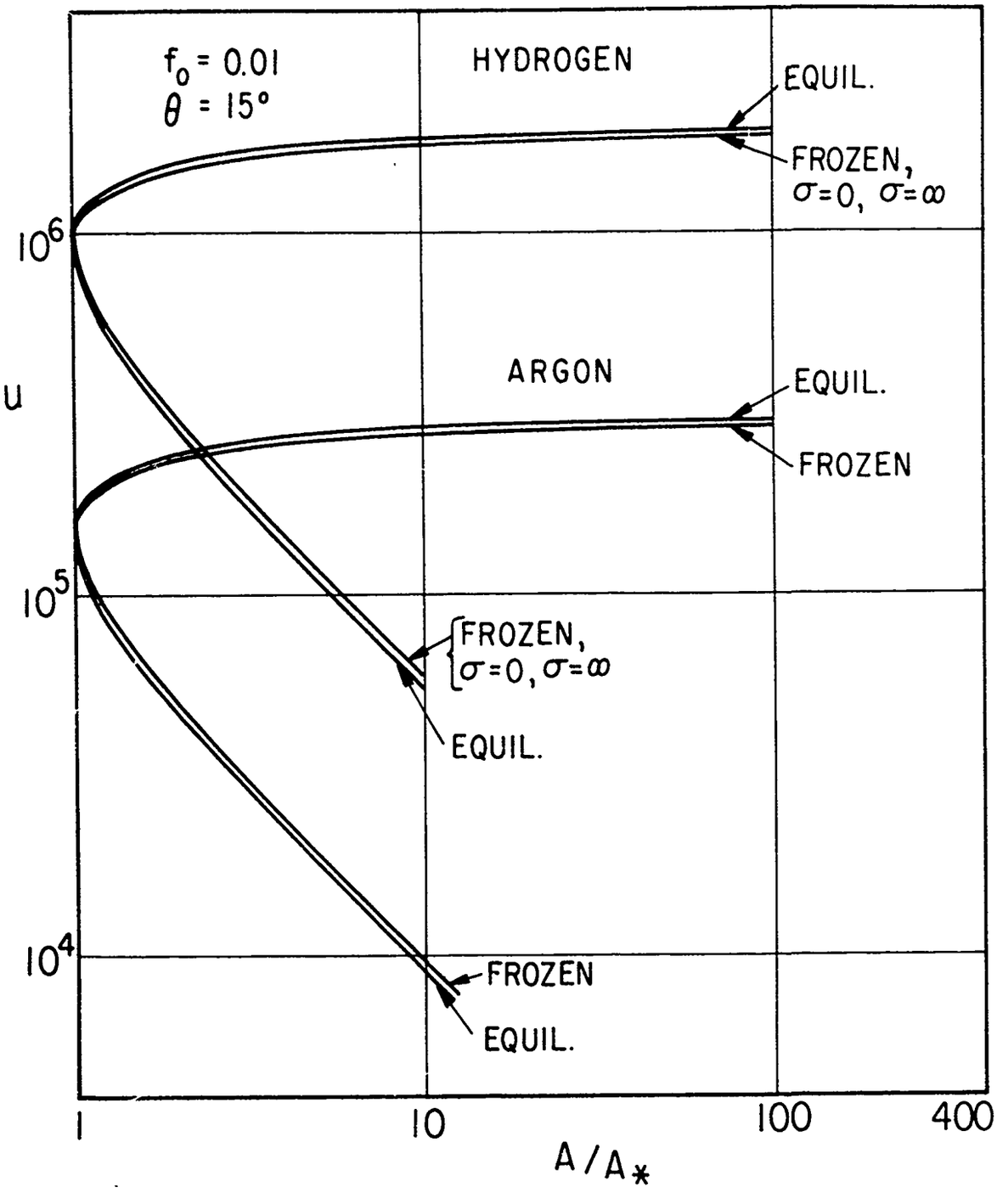

FIG. 4b VELOCITY (cm/sec)

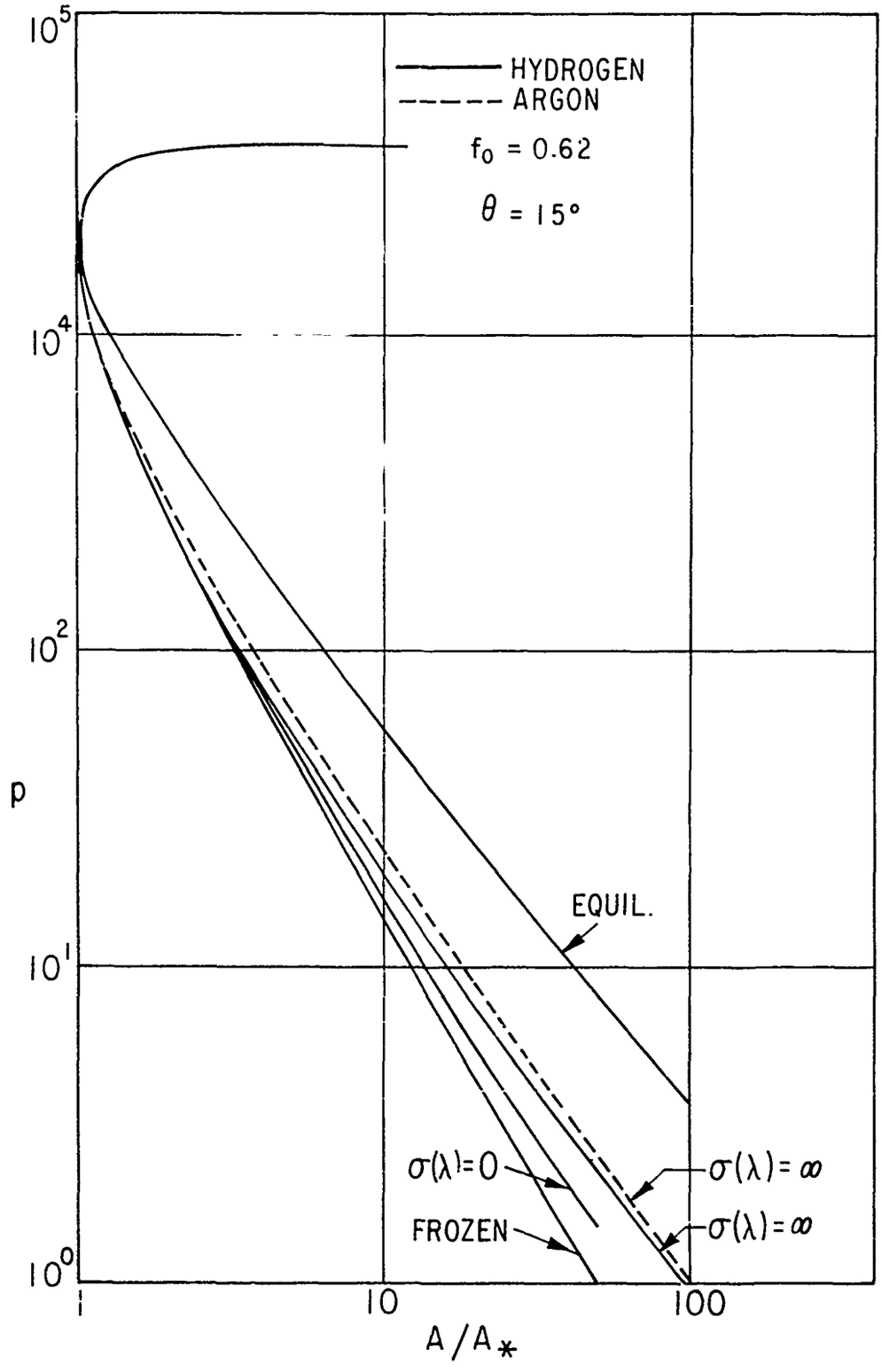

FIG. 5a PRESSURE, (dynes/cm^2)

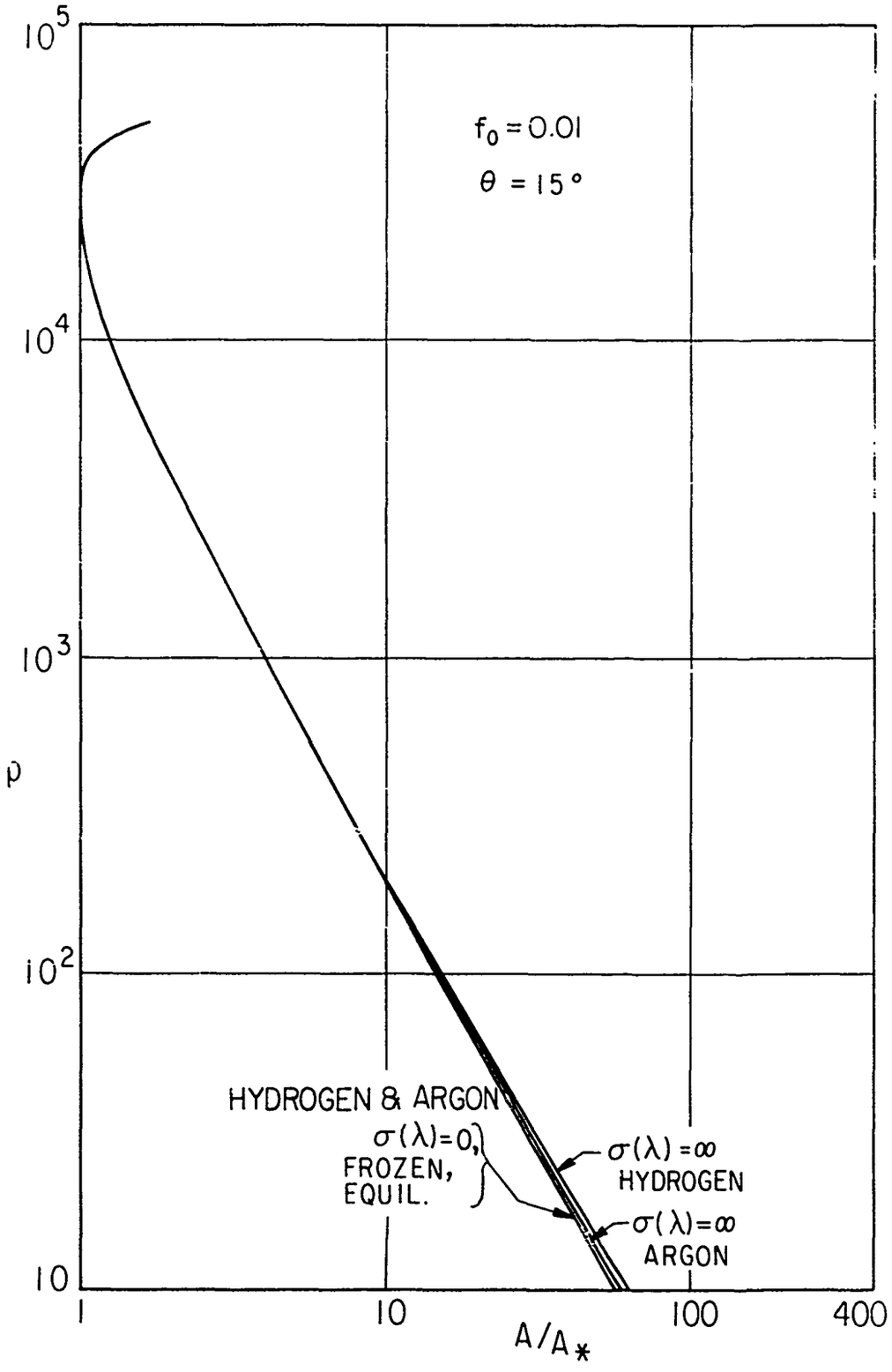

FIG. 5b PRESSURE (dynes/cm^2)

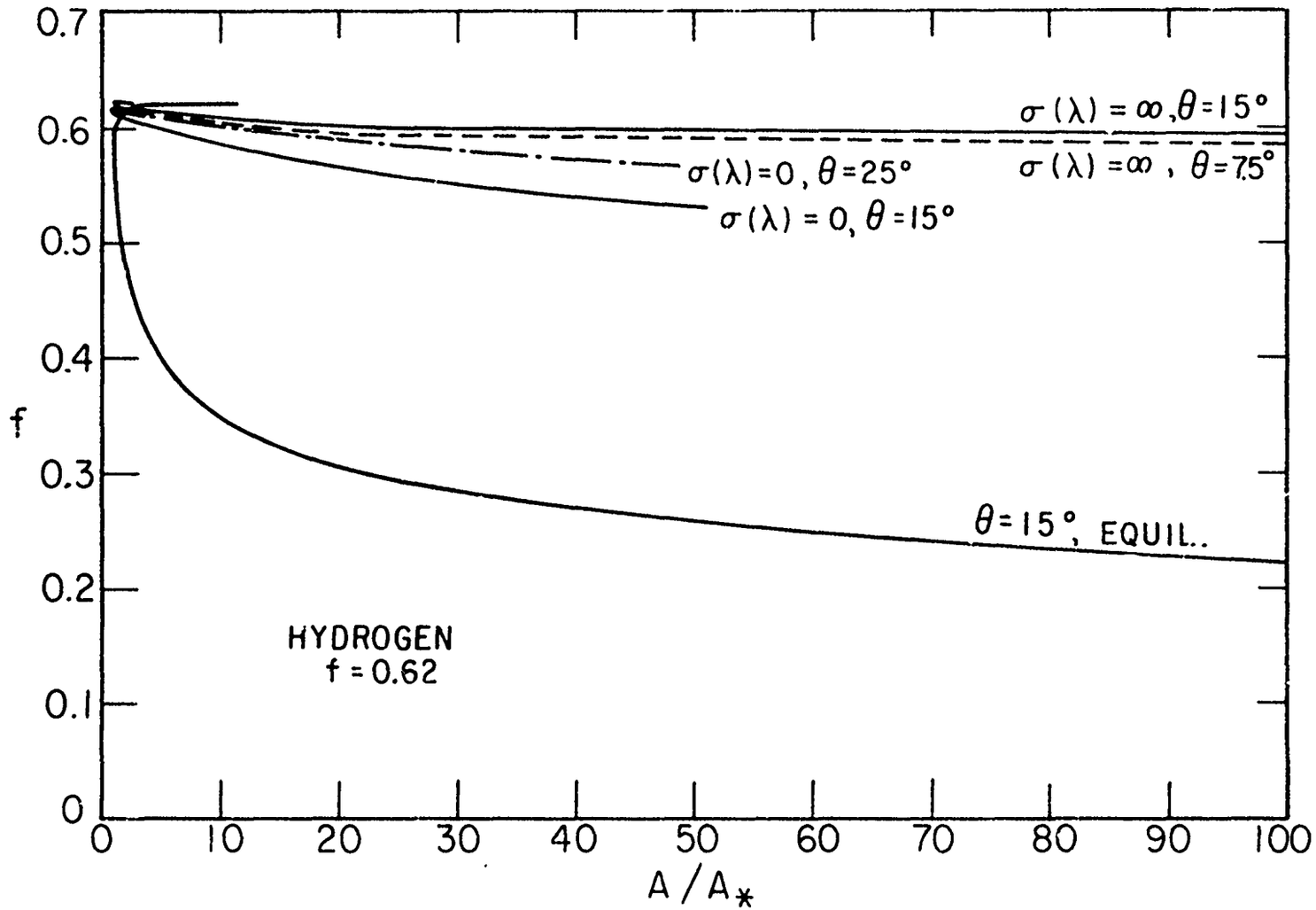

FIG.6 DEGREE OF IONIZATION

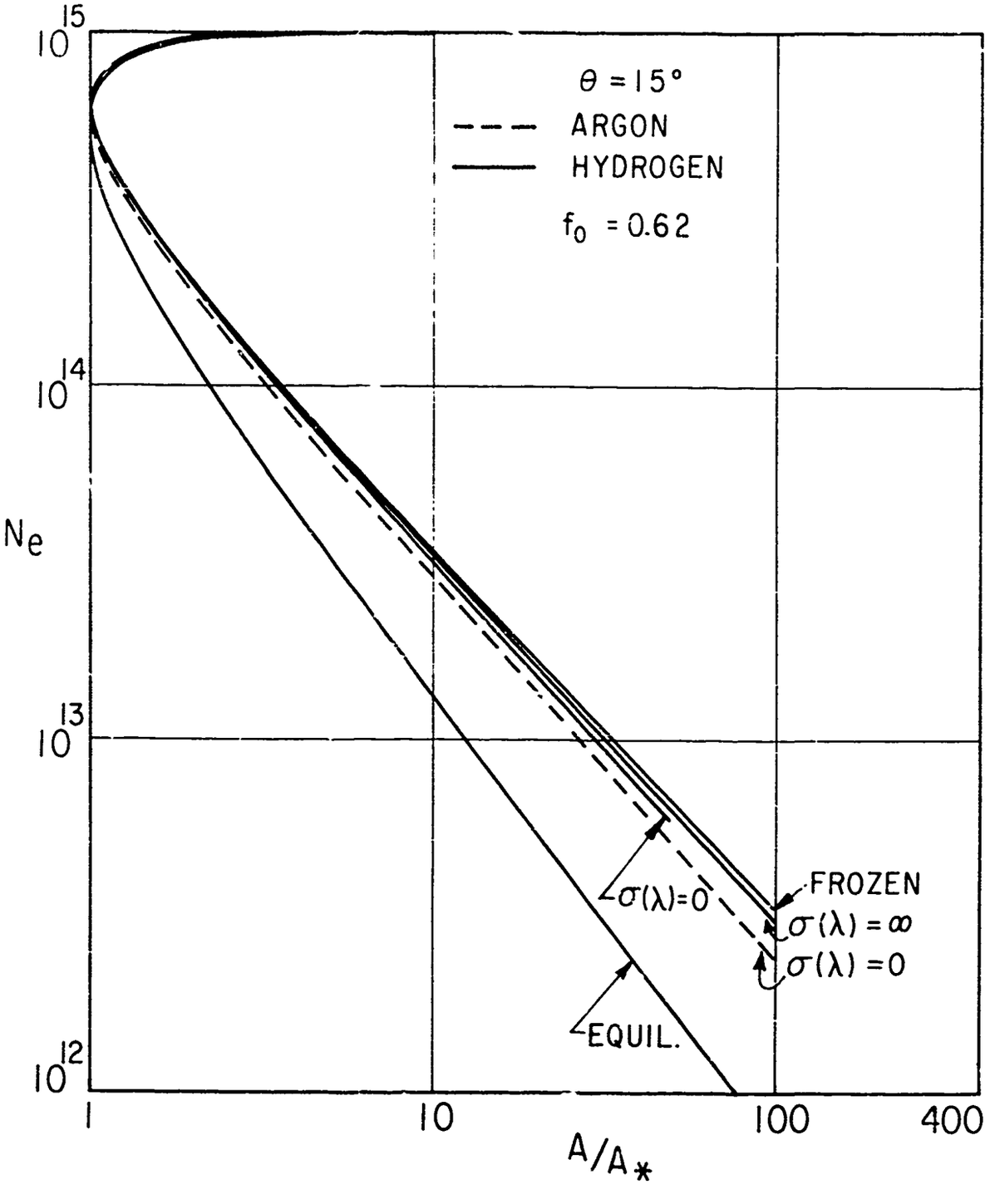

FIG. 7a ELECTRON NUMBER DENSITY

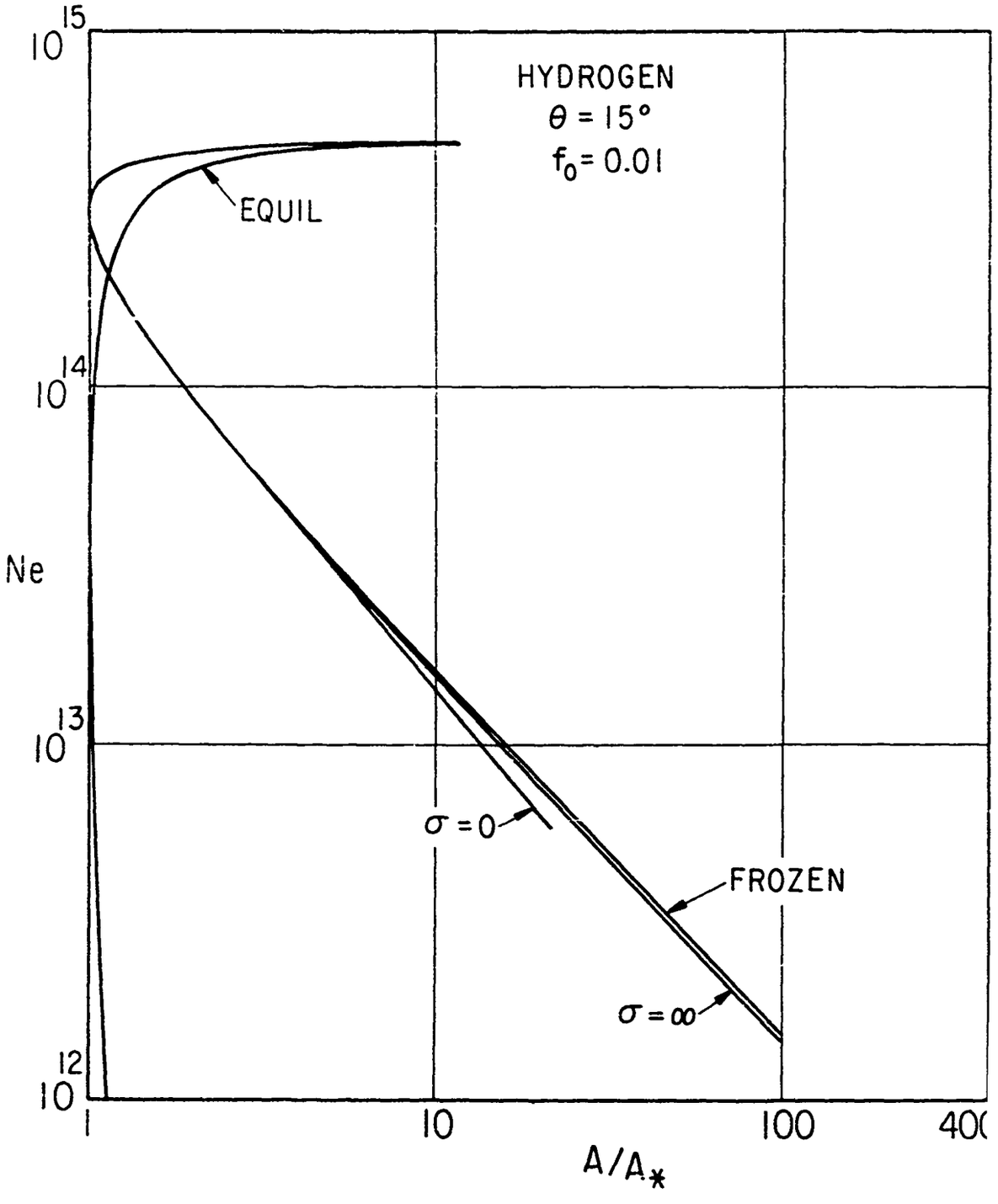

FIG. 7b ELECTRON NUMBER DENSITY

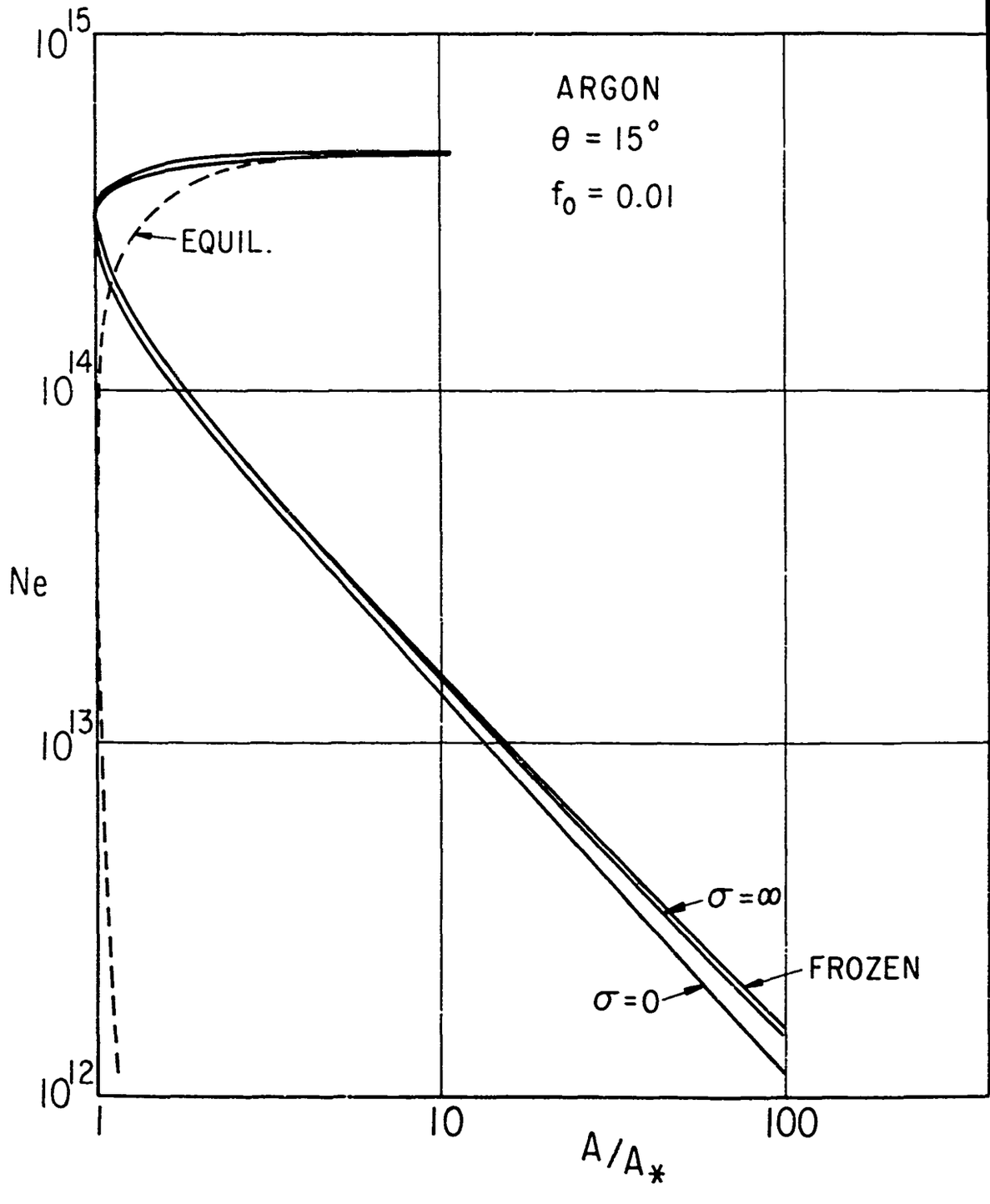

FIG. 7c ELECTRON NUMBER DENSITY

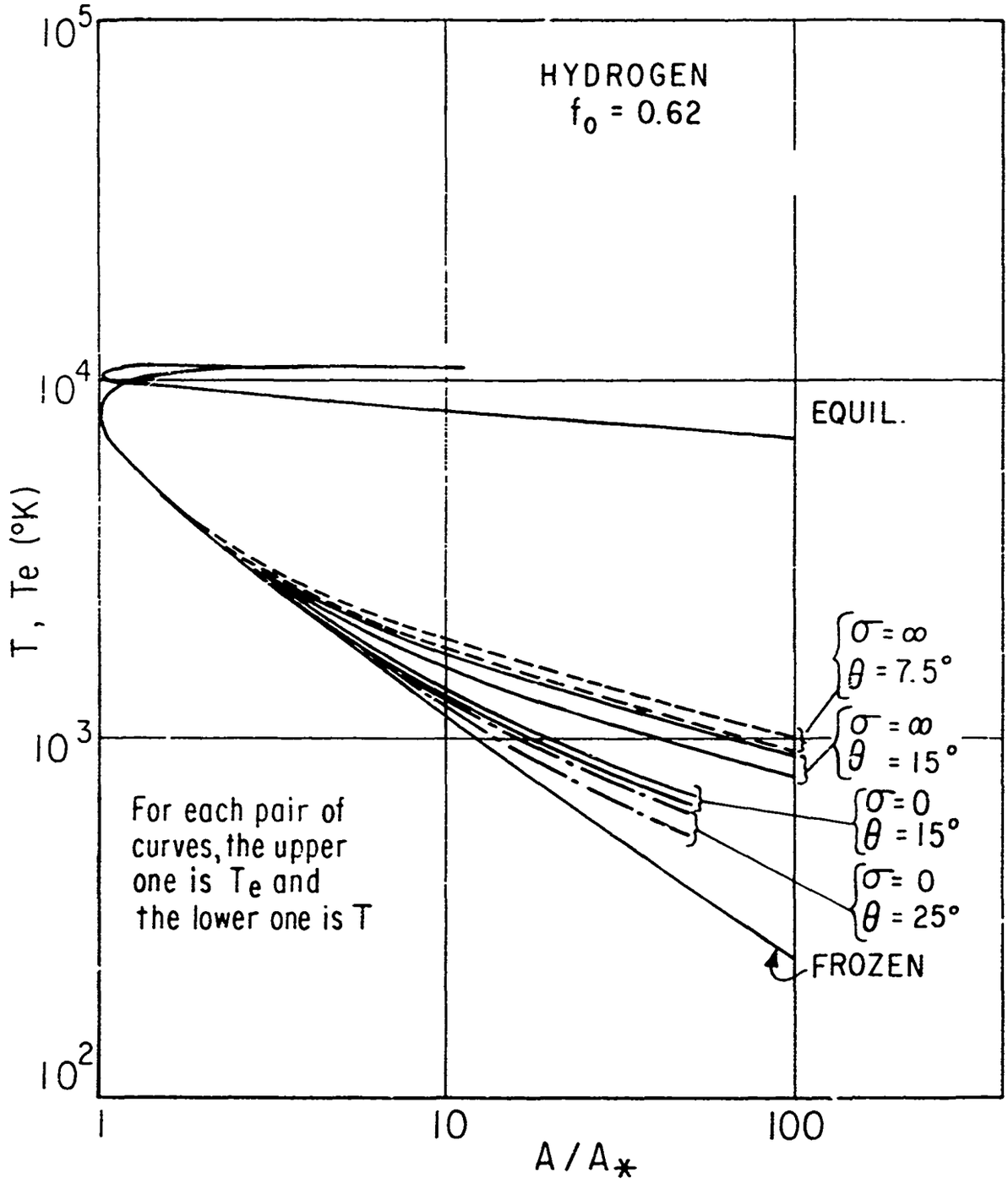

FIG. 8a TEMPERATURES

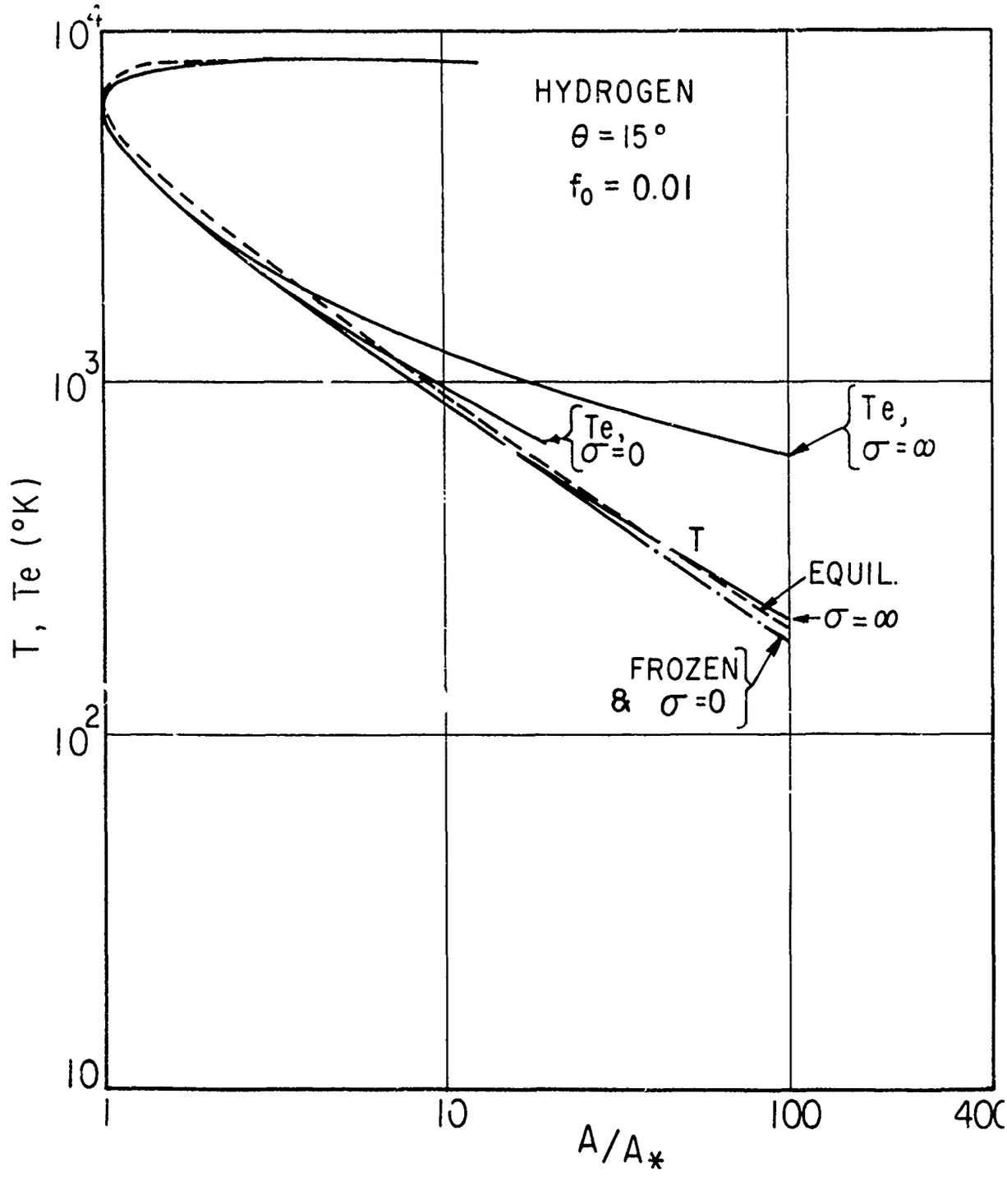

FIG. 8b TEMPERATURES

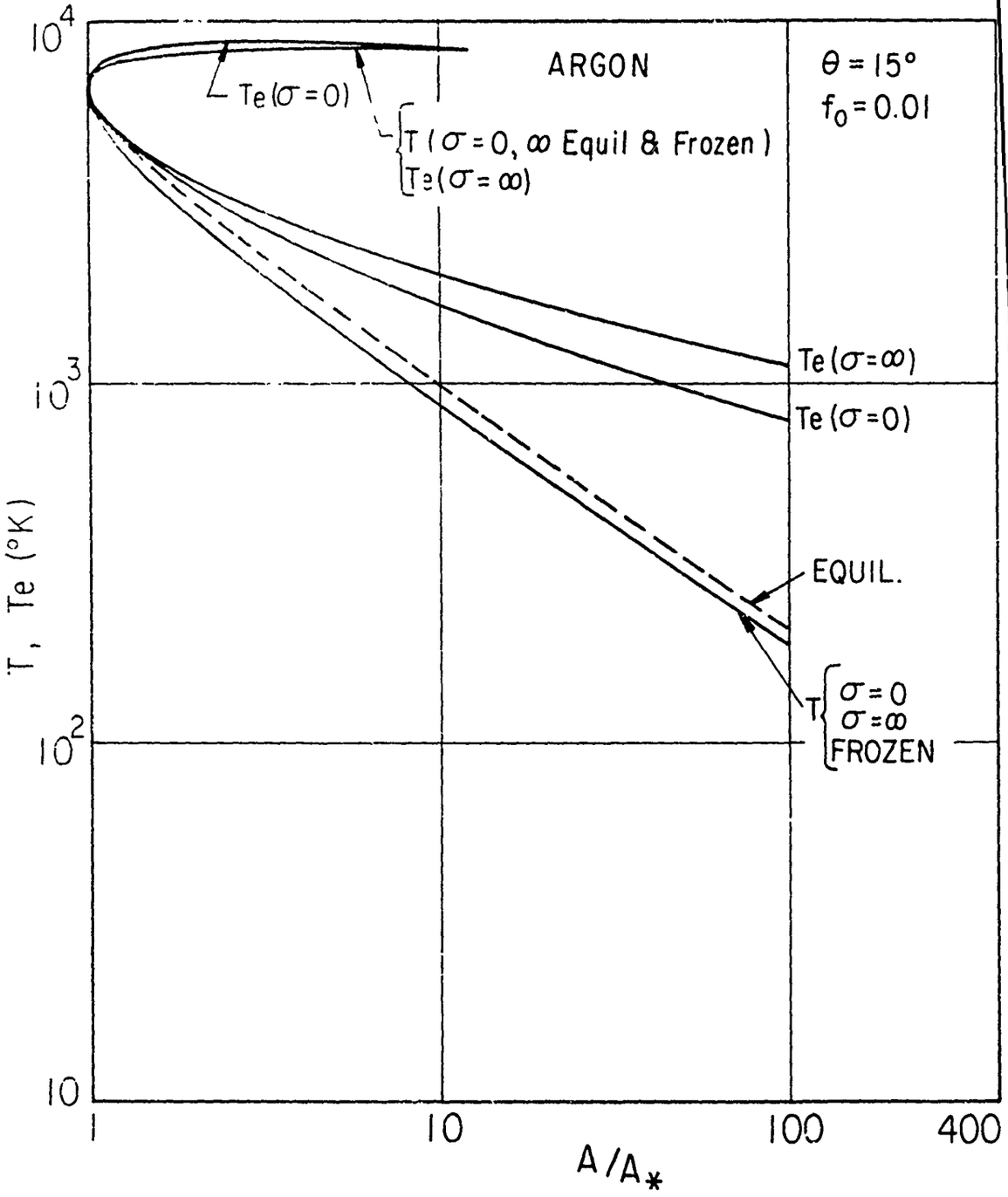

FIG. 8c TEMPERATURES

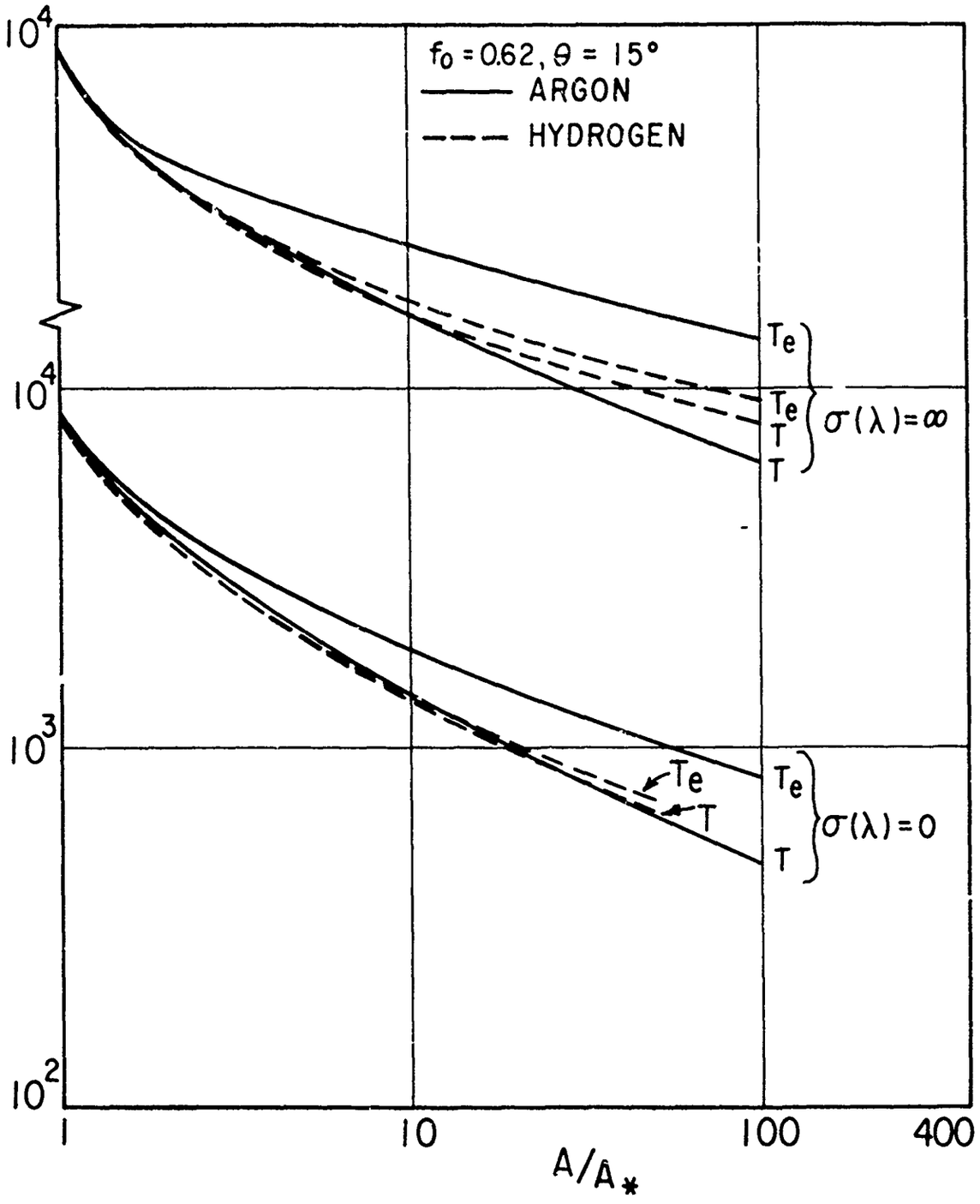

FIG. 9 TEMPERATURES

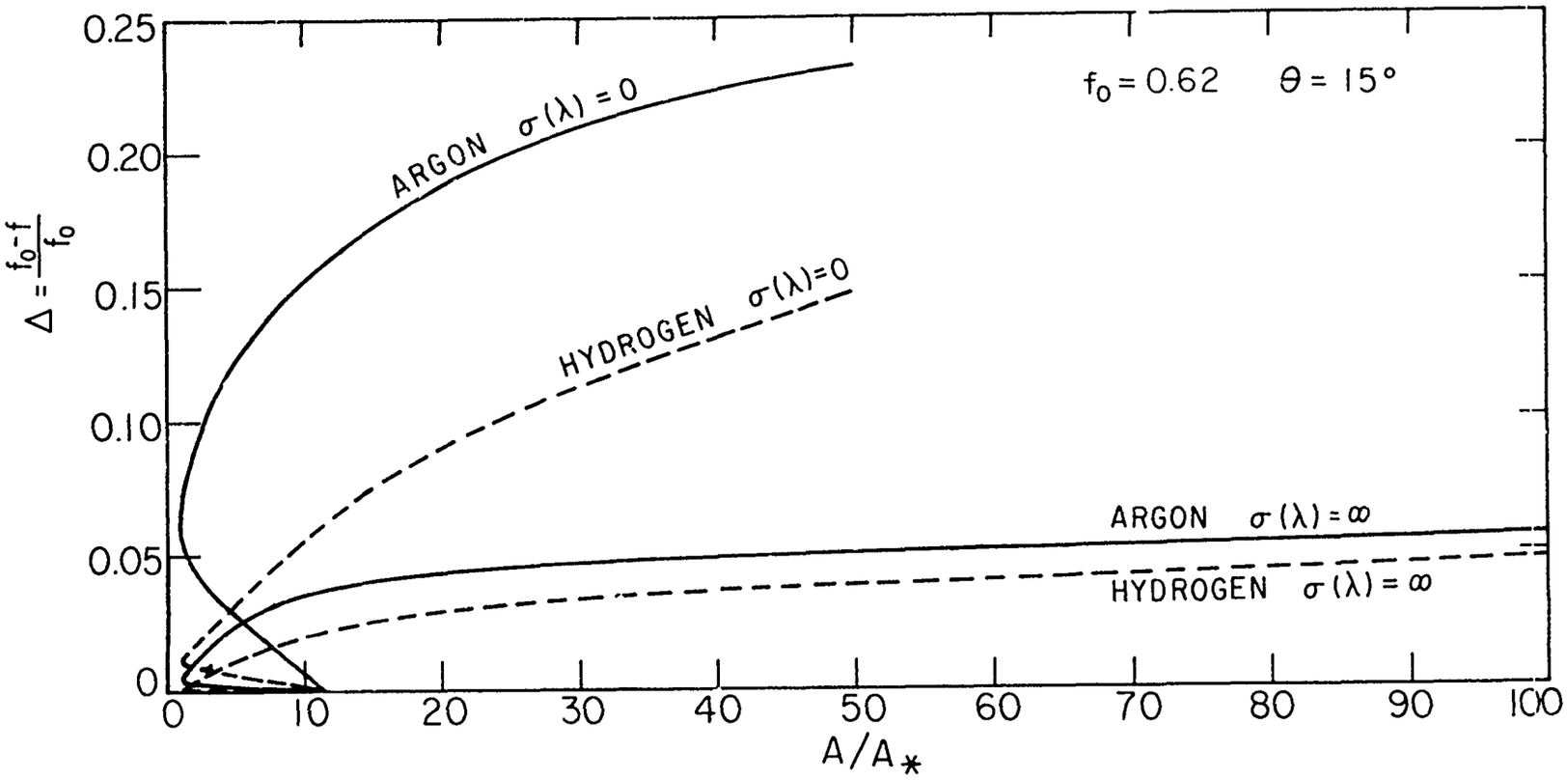

FIG. 10a FRACTIONAL IONIZATION CHANGE

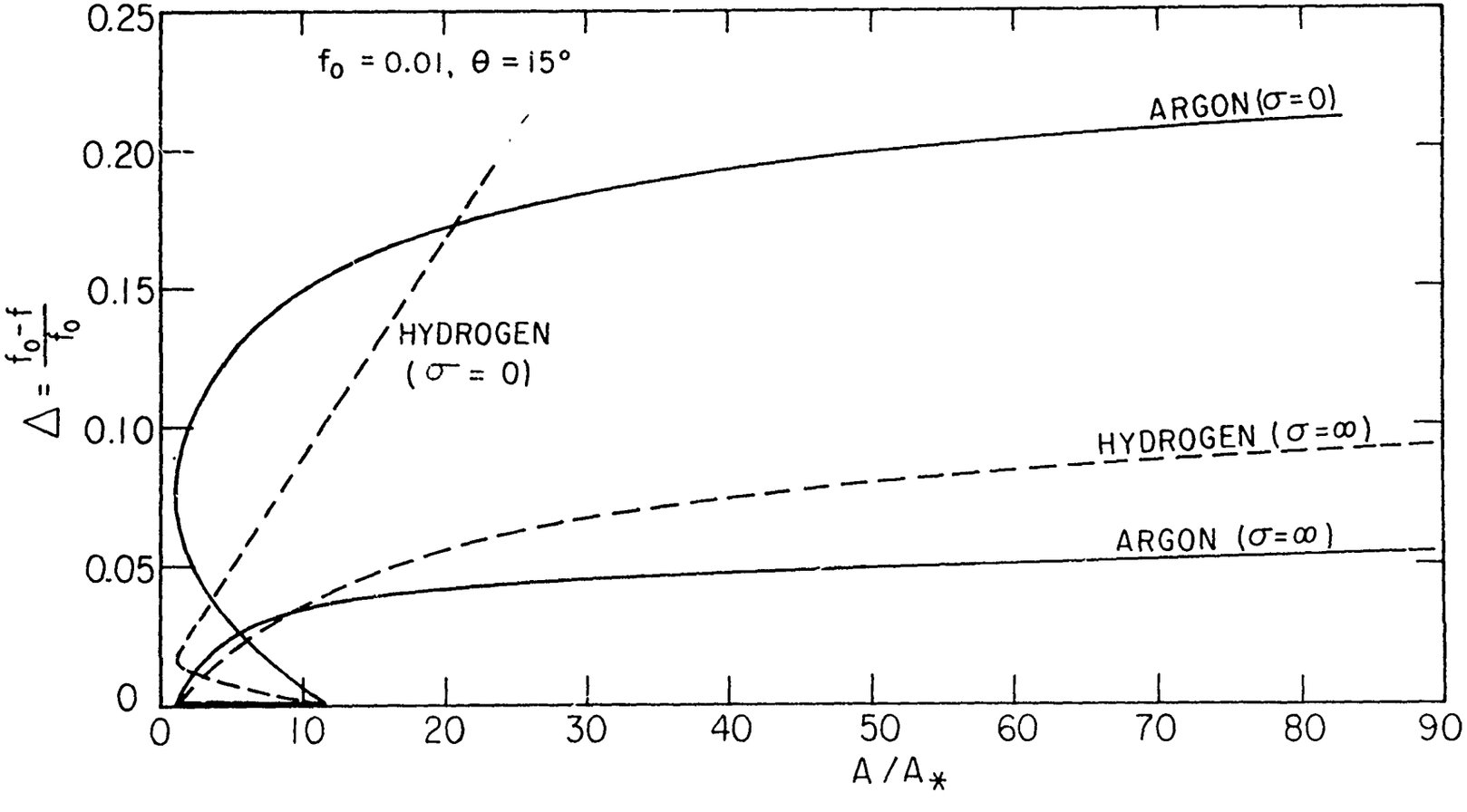

FIG. 10b FRACTIONAL IONIZATION CHANGE

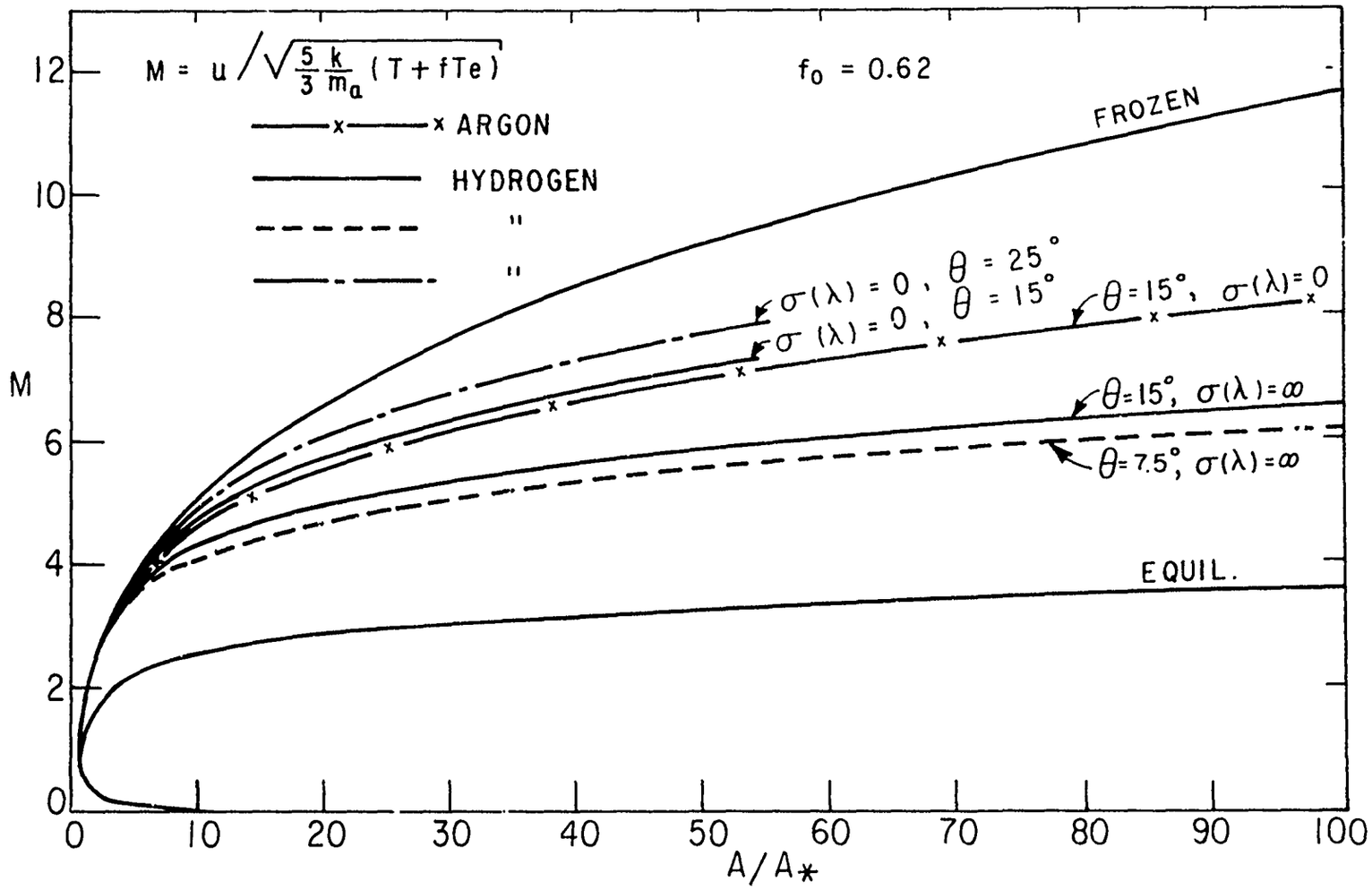

FIG. IIa MACH NUMBER

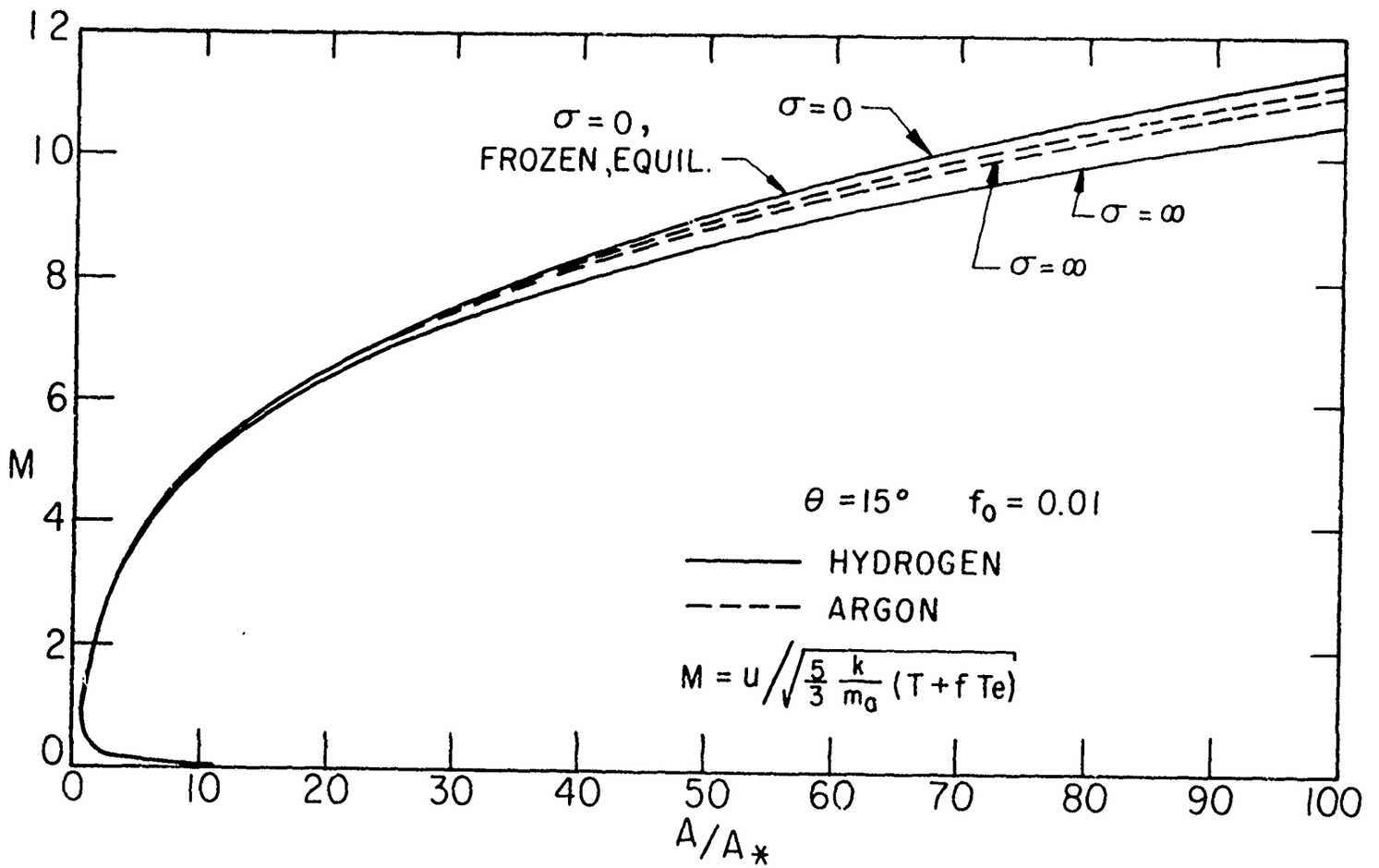

FIG. 11b MACH NUMBER

UNCLASSIFIED

Security Classification

DOCUMENT CONTROL DATA - R&D

(Security classification of title, body of abstract and indexing annotation must be entered when the overall report is classified)

1 ORIGINATING ACTIVITY (Corporate author) University of California	2a REPORT SECURITY CLASSIFICATION UNCLASSIFIED 2b GROUP

3 REPORT TITLE

Expansion of a Partially-Ionized Gas Through a Supersonic Nozzle

4 DESCRIPTIVE NOTES (Type of report and inclusive dates)

Technical Report

5 AUTHOR(S) (Last name, first name, initial)

Talbot, L., Chou, Y. S., Robben, F.

6 REPORT DATE	7a TOTAL NO OF PAGES	7b. NO OF REFS
August 1965	32	22

8a CONTRACT OR GRANT NO. AFOSR Grant 538-65 b PROJECT NO. c. d	9a ORIGINATOR'S REPORT NUMBER(S) AS-65-14 9b. OTHER REPORT NO(S) (Any other numbers that may be assigned this report)

10 AVAILABILITY/LIMITATION NOTICES

Qualified requesters may obtain copies of this report from DDC.

11. SUPPLEMENTARY NOTES	12 SPONSORING MILITARY ACTIVITY
	Air Force Office of Scientific Research

13 ABSTRACT

A theoretical investigation was made of the non-equilibrium expansion of a partially ionized gas through a supersonic nozzle. Both hydrogen and argon were studied. The ionization and recombination rate parameters used were those calculated by Bates and co-workers, using their collisional-radiative model of the recombination process. These calculations, for hydrogen, include the influence of radiation trapping on the overall rates, and yield as well the amount of recombination energy which is gained by the third-body electron in the recombination.

The energy balance for the electrons and massive particles was studied for both the optically thin (all recombination radiation lost) and optically thick (all radiation absorbed) cases. It was found that the recombination process produces an increase in electron temperature over that of the ion-atom temperature, and that this temperature difference is greater for the optically thick than for the optically thin case. Also, there is more net recombination for the optically thin case.

For high initial ionization (62%), recombination affects the gross flow variables measurably, when compared with the "frozen flow" solution. For low initial ionization (1%) the gross flow variables are practically unaltered, and the principal effect of the recombination is to produce an elevated electron temperature.

On comparing the hydrogen and argon flows, one finds that the effect of the larger atomic mass of the argon is to diminish the effectiveness of electron-atom energy exchange, resulting in a larger difference between electron and atom temperatures.

DD FORM 1 JAN 64 1473

UNCLASSIFIED

Security Classification